CONFIDENTIAL

FINAL REPORT
on the
VHF FERRITE ANTENNA DEVELOPMENT PROGRAM

April 30, 1957

REFERENCE: [redacted] 25X1

[redacted] 25X1

CONFIDENTIAL

Final Report on the
VHF FERRITE ANTENNA DEVELOPMENT PROGRAM

I. INTRODUCTION

The objective of the VHF ferrite antenna development program was to study the possible advantages offered by the use of ferrite materials in antennas from 3 to 30 mc/s. It was felt that ferrite materials had the potential of improving antenna performance by virtue of their high permeability, low losses, and dispersive effects. The high permeability and low losses were to produce increased gain by providing greater coupling to the radiating fields. The dispersion of permeability was to result in increased bandwidth. This report summarizes the results of the study with particular emphasis placed on the work done in the period from January 1 to May 31, 1957.

II. RESULTS AND CONCLUSIONS

The present study of ferrite antennas was confined to small antennas having maximum dimensions much less than a wavelength. The following conclusions were formed during the study and apply to such small antennas.

The diameter of a loop antenna can be reduced without a loss in gain or sensitivity by adding a ferrite core, but the required length of ferrite rod will be greater than the diameter of the original loop. If the maximum dimensions of the two antennas are to be made equal, the gain of the air-core loop will be greater than the gain of a ferrite core loop.

Expressions were derived comparing the sensitivity of a ferrite antenna with an air-core loop in the presence of antenna thermal noise. Similar conclusions were reached[2]; the diameter of the loop could be reduced by adding a ferrite core without a loss in sensitivity, provided the length of the core was greater than the diameter of the original loop. The results were not verified expermentally, for the receiver

noise not antenna noise was found to limit sensitivity. When receiver noise dominates, it is simply antenna gain which governs sensitivity.

The ferrite antenna will be more convenient to package than the air loop in certain applications. The ferrite antenna has its maximum dimension in only one direction. The resulting line geometry will at times be an advantage over the plane geometry of an air loop.

A monopole antenna, like the ferrite antenna, also has a line geometry. Nevertheless, the ferrite antenna will at times have packaging advantages even over the monopole. The monopole must be situated perpendicular to a ground plane; e.g., the chassis. The ferrite rod can be placed parallel to the chassis. Therefore, the ferrite antenna inherently allows a more compact package. However, the use of monopoles has been extended by simple designs that allow convenient stowing; e.g., telescoping rods or wire wound on a reel.

A small loop antenna with a ferrite core was found to produce a greater terminal voltage in the 3 - 30 mc/s range than a monopole antenna of the same size. However, the induced voltage, in contrast to the terminal voltage, was greater for the monopole. The performance of the monopole was degraded by the coupling network which was of conventional design for a capacitively tuned antenna. If the property of convenient stowing allowed a monopole to be used greater in length than the ferrite rod, the performance of the monopole could be made comparable to or better than the performance of the loop.

The voltage per turn induced in a loop decreases 20 db/decade with the frequency. However, when the antenna is designed for a lower operating frequency, the number of turns on the loop can be increased. For a fixed range of tuning capacitance, the allowed number of turns is inversely proportional to the center frequency, exactly compensating for the reduced voltage per turn. Therefore, the net induced voltage is in effect nearly constant at different center frequencies for a loop antenna

similar to the monopole antenna. The additional windings will also add stray capacitance, preventing exact compensation at low frequencies.

No advantages were found using the dispersive effects of ferrites in small antennas. The dispersion was too weak and the losses too great in the dispersive region. Theory indicates that the behavior required of the complex permeability for wide-band operation is not physically realizable over a broadband of frequencies. No attempt to develop improved dispersive material should be initiated without first giving due consideration to this theory.

The most fruitful improvement in ferrite materials appears to be an extension of their useful range into higher frequencies. Materials are not available which have high permeability and quality factors above 30 mc/s. On the other hand, it does not appear fruitful to develop extremely high permeability materials for small antennas. The intrinsic permeability becomes ineffective for producing improved performance in small antennas with ferrite cores of reasonable length-to-diameter ratios.

No evidence was found to indicate that the loop antenna would be less susceptible to interference or proximity effects than a monopole antenna. Rather, when both antennas are considered coupled to the electric field, no fundamental difference between the two antennas is apparent. Details do differ, however, and design parameters should be chosen to favor the particular type antenna chosen.

Dielectric materials are not expected to yield greater advantages than do the magnetic materials in small antennas. The theoretical treatment of the dielectric antenna would be very similar to the treatment of the ferrite antenna. For example, there is a de-polarization factor for a dielectric rod which corresponds precisely to the demagnetization factor for the magnetic rod. Also, the theoretical treatment of complex permeabilities is directly applicable to complex permittivities.

There is a severe fundamental limitation on the gain-bandwidth product of small antennas which is described in a theory by Chu[1]. The gain of an antenna much

smaller than a wavelength which is designed for a maximum gain-bandwidth product nearly equals the gain of a half-wave dipole; but the bandwidth becomes vanishingly small as the size of the antenna is reduced.

III. RECOMMENDATIONS

Ferrite core loop antennas should be used in applications where a compact package is required. More convenient packaging is the principal advantage provided by the ferrite antennas.

Improved magnetic materials should be developed for application to small antennas above 30 mc/s. High permeability, low loss materials are needed. Studies should be made of the advantages using ferrites in antennas comparable in size to a wavelength. There will be a better utilization of the magnetic properties of the materials in these large antennas than in small antennas. Furthermore, it is likely that small dispersive effects can be accumulated and used to an advantage in large antennas. If small dispersive effects can be used, the accompanying losses need not be prohibitively large. Small dispersive effects accumulated over many wavelengths are already being used in microwave and optical applications; e.g., microwave ferrite phase shifters and achromatic lenses.

IV. PROGRESS

A. COMPLEX PERMEABILITY

1. Intrinsic Permeability

a. Concepts

The VHF ferrite antenna consists of a conducting coil wound on a ferrite core. The ferromagnetic properties of the core material are described by its permeability, "μ". The permeability is the ratio of the magnetic flux density to the magnetic field intensity

$$\overline{B} = \mu_i \overline{H} \qquad (1)$$

The resistivity of ferrite materials can be made very large resulting in negligible conduction losses. In such cases, the core losses are principally hysteresis losses.

The hysteresis loss is proportional to the area enclosed by the hysteresis loop. See Figure 1

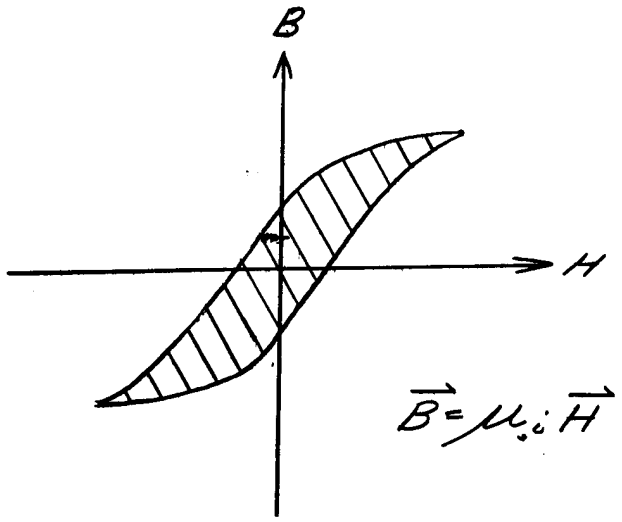

FIGURE 1
LARGE SIGNAL HYSTERESIS LOOP

It is shown in Appendix A that, for complex permeabilities,

$$\mu_i = \mu_i' - j\,\mu_i'' \qquad (2)$$

the hysteresis loop is approximated by an ellipse. See Figure 2. The approxi-

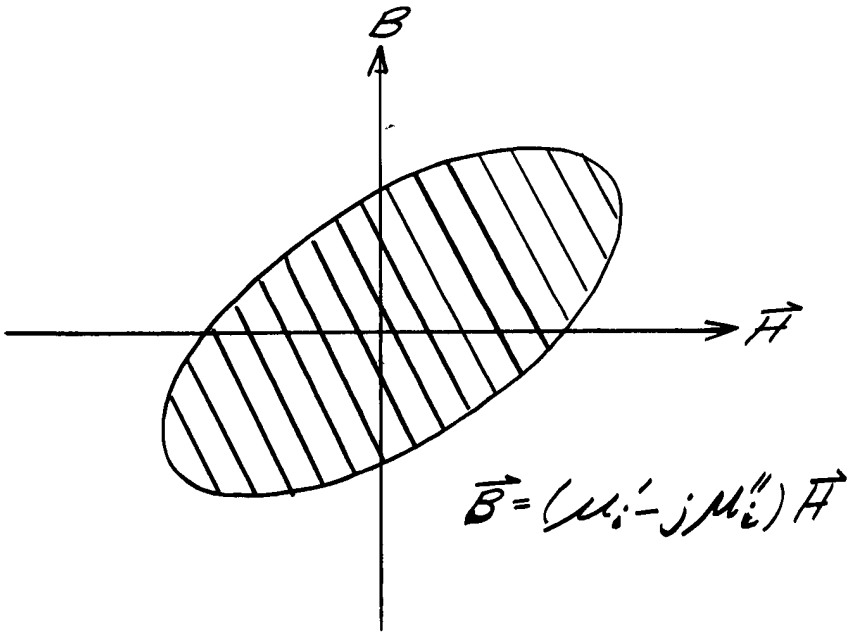

FIGURE 2
SMALL SIGNAL HYSTERESIS LOOP

mation is valid for small field intensities. The imaginary part of the complex permeability is responsible for the hysteresis losses. When $\mu_i'' = 0$, the hysteresis loop degenerates into a straight line. The area enclosed by the loop vanishes, and no losses occur.

The complex permeability is a function of frequency. For example, the real permeability decreases markedly at high frequencies. The magnetic domains simply do not have sufficient time to align themselves with the field before the field reverses itself. The decrease in permeability at high frequencies is called the dispersion of permeability. At the same frequencies, where the material becomes dispersive, the hysteresis losses become large.

b. Measurements

The complex permeabilities of several ferrites were measured from 3 to 30 Mc/s. The permeabilities were derived from impedance measurements. Both

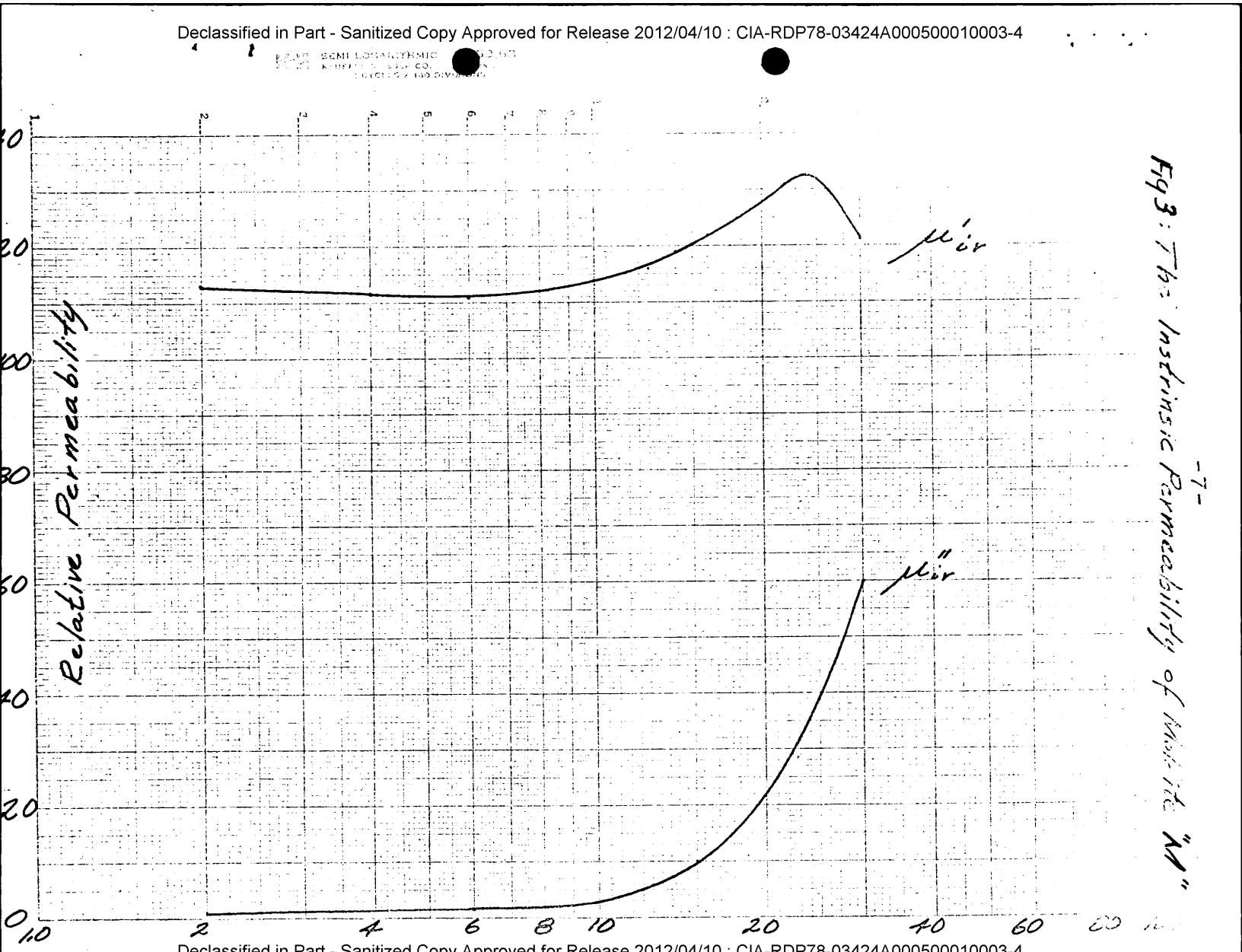

Fig 3: The Instrinsic Permeability of Mn-Zn "M"

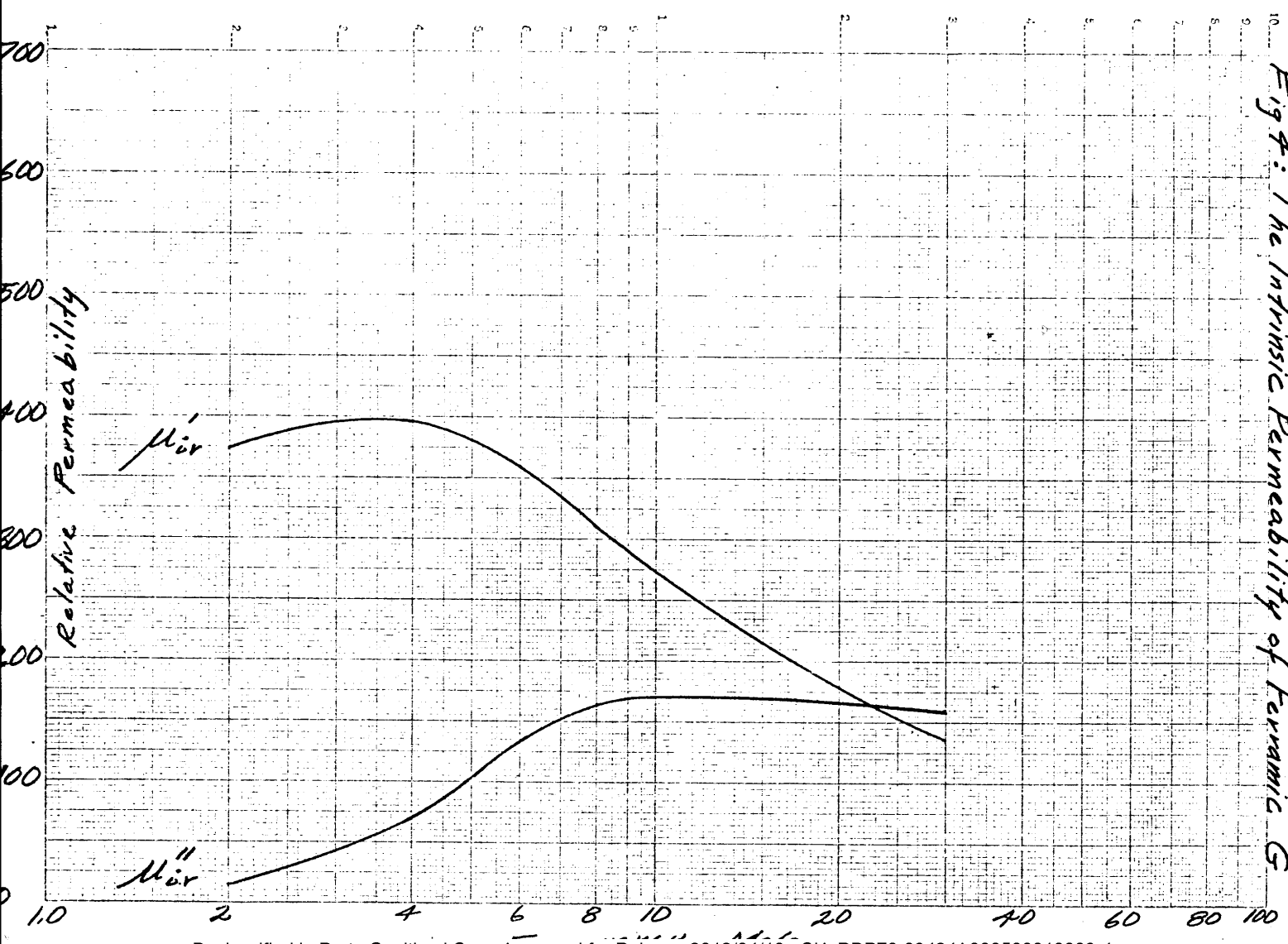

Fig 4: The Intrinsic Permeability of Ferramic "G"

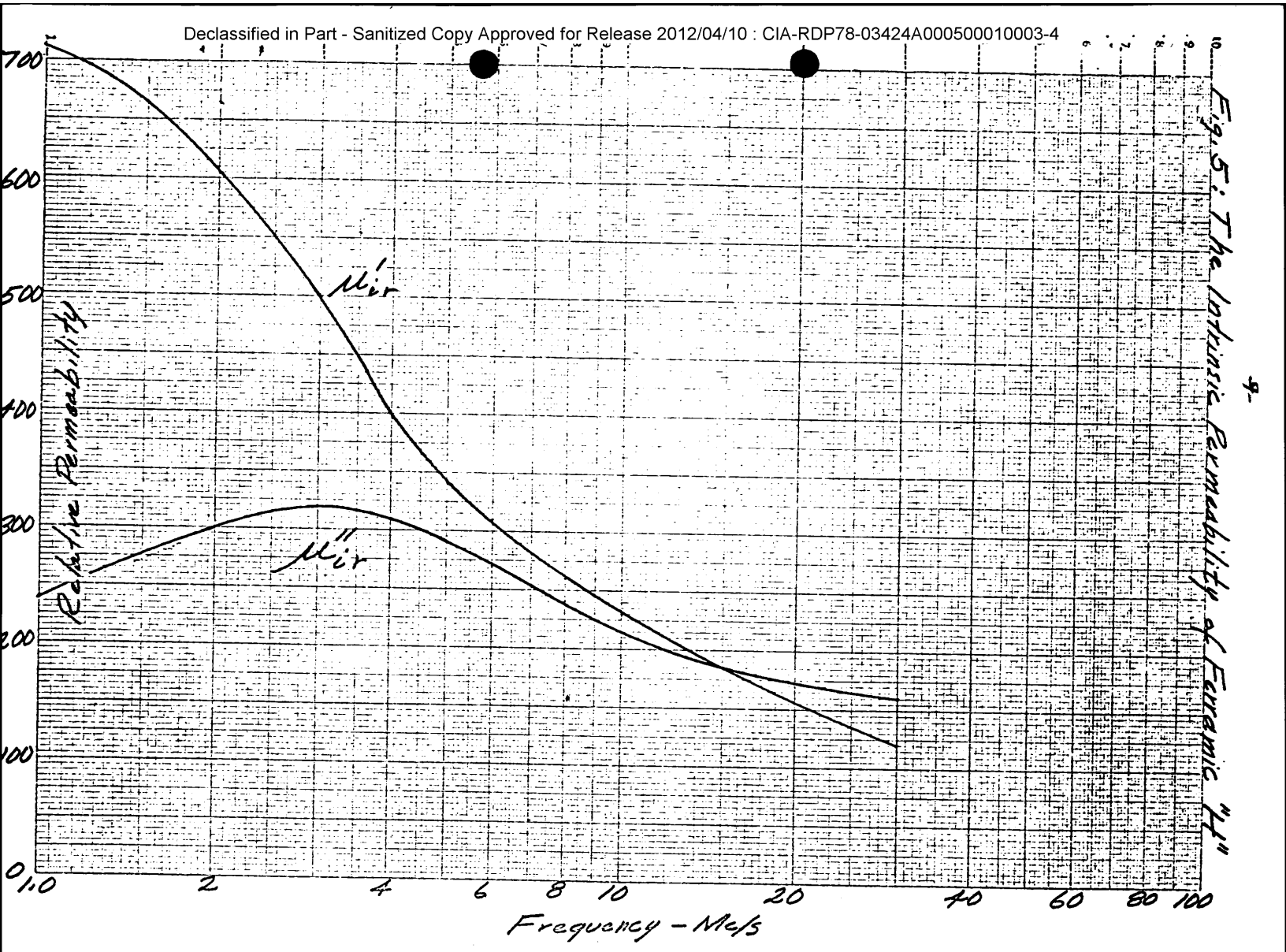

Fig. 5: The Intrinsic Permeability of Ferramic "H"

a ferrite-loaded coaxial waveguide and a ferrite-cored toroidal coil were used. The analyses required to derive the permeability from the impedance measurements are included in Appendices B and C. The results for Moldite "M", Ferramic G, and Ferramic H are presented graphically in Figures 3, 4, and 5. Note that the greater the d.c. permeability, the lower the frequency where dispersion occurs. Note also that the greatest losses occur in the region of dispersion.

2. Effective Permeability

The permeability defined in the previous sections is an intrinsic property of the material. For emphasis, it is termed the intrinsic permeability. It is the intrinsic permeability which appears in Maxwell's equations and in their solutions.

After a solution is found to Maxwell's equations, it is sometimes convenient to define an "effective permeability" which is a function of both the intrinsic properties and the geometry of the material. For example, consider a small prolate spheroid of ferrite material placed in a uniform magnetic field with its axis parallel to the direction of the field. The quasi-static solution of the field equations reveals that the magnetic field inside the ferrite is also uniform(1)

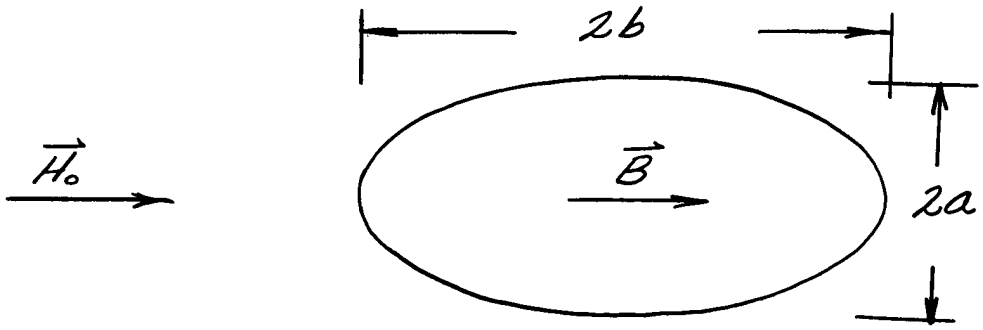

FIGURE 6
OBLATE SPHEROID IN A UNIFORM MAGNETIC FIELD

An effective permeability can be defined such that the flux density within the material is proportional to the strength of the original field and the effective permeability of the spheroid

$$\bar{B} = \mu_e \bar{H}_o \tag{3}$$

The effective permeability is a function of the intrinsic permeability and the geometry of the material.

$$\mu_e = \mu_o \frac{\mu_{ir}}{1 + D(\mu_{ir} - 1)} \tag{4}$$

where

μ_o = permeability of free space.

μ_{ir} = relative intrinsic permeability of the ferrite material.

D = demagnetization factor along the axis of the spheroid.

The demagnetization factor is a function of geometry alone and, for the prolate spheroid, becomes

$$D = \frac{e^2}{1-e^2}\left[\frac{1}{2\sqrt{1-e^2}} \ln \frac{1+\sqrt{1-e^2}}{1-\sqrt{1-e^2}} - 1\right] \tag{5}$$

The eccentricity is

$$e = b/a$$

By considering the analogous expression for oblate spheroids, it can be seen that

for needles $D \longrightarrow 0$

for discs $D \longrightarrow 1$

Since the intrinsic permeability is complex and a function of frequency, the effective permeability is also complex and frequency dependent

$$\mu_e = \mu_e' - j\,\mu_e'' \tag{6}$$

For the prolate spheroid, the effective relative permeabilities are

$$\mu_{er}' = \frac{\mu_{ir}'\left[1 + D(\mu_{ir}' - 1)\right] + D\,(\mu_{ir}'')^2}{\left[1 + D(\mu_{ir}' - 1)\right]^2 + \left[D\,\mu_{ir}''\right]^2} \tag{7}$$

and

$$\mu_{er}'' = \frac{\mu_{ir}''\,(1 - D)}{\left[1 + D(\mu_{ir}' - 1)\right]^2 + \left[D\,\mu_{ir}''\right]^2} \tag{8}$$

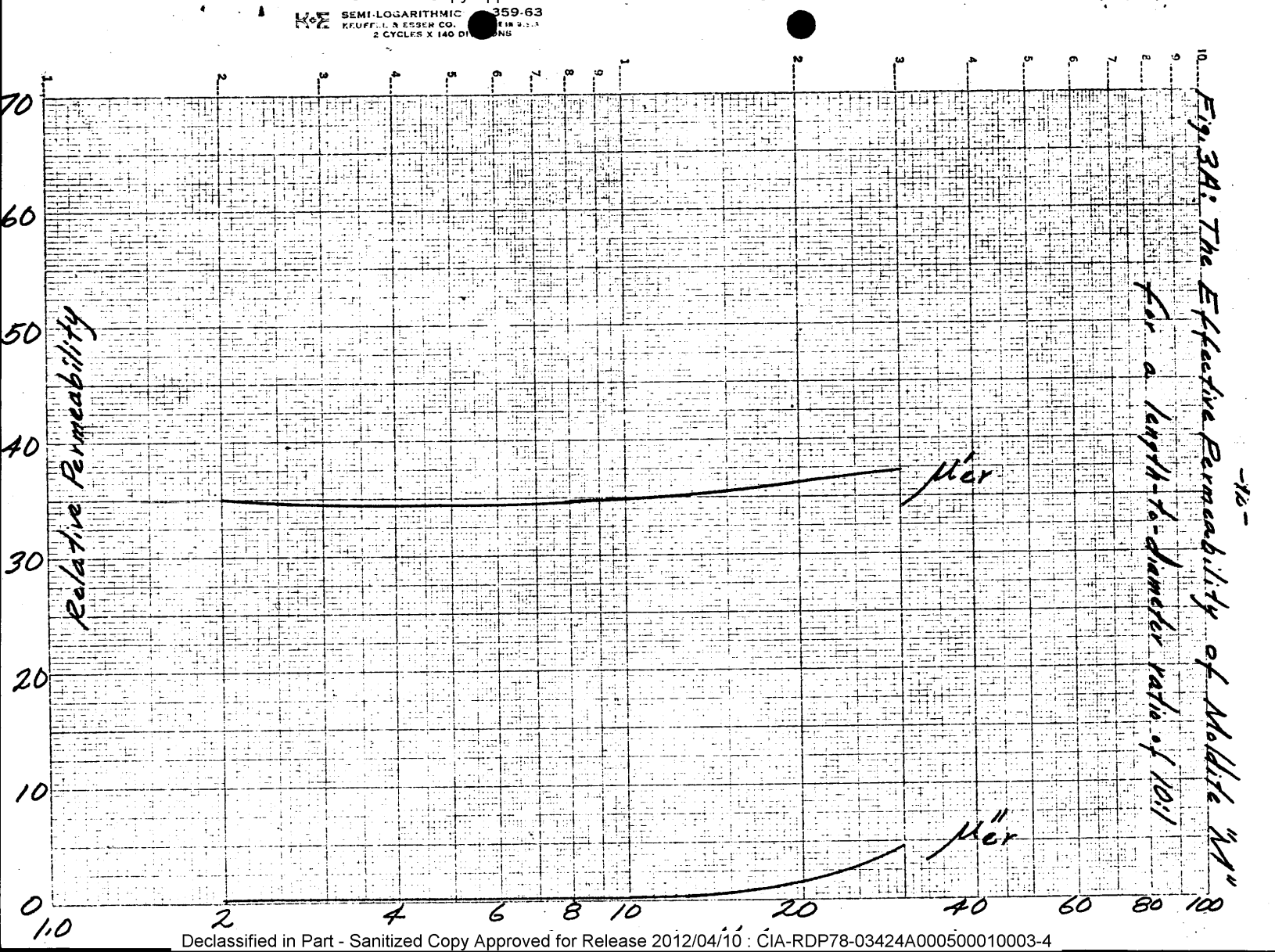

Fig. 3A: The Effective Permeability of Molybdenum Permalloy for a Length-to-diameter ratio of 10:1

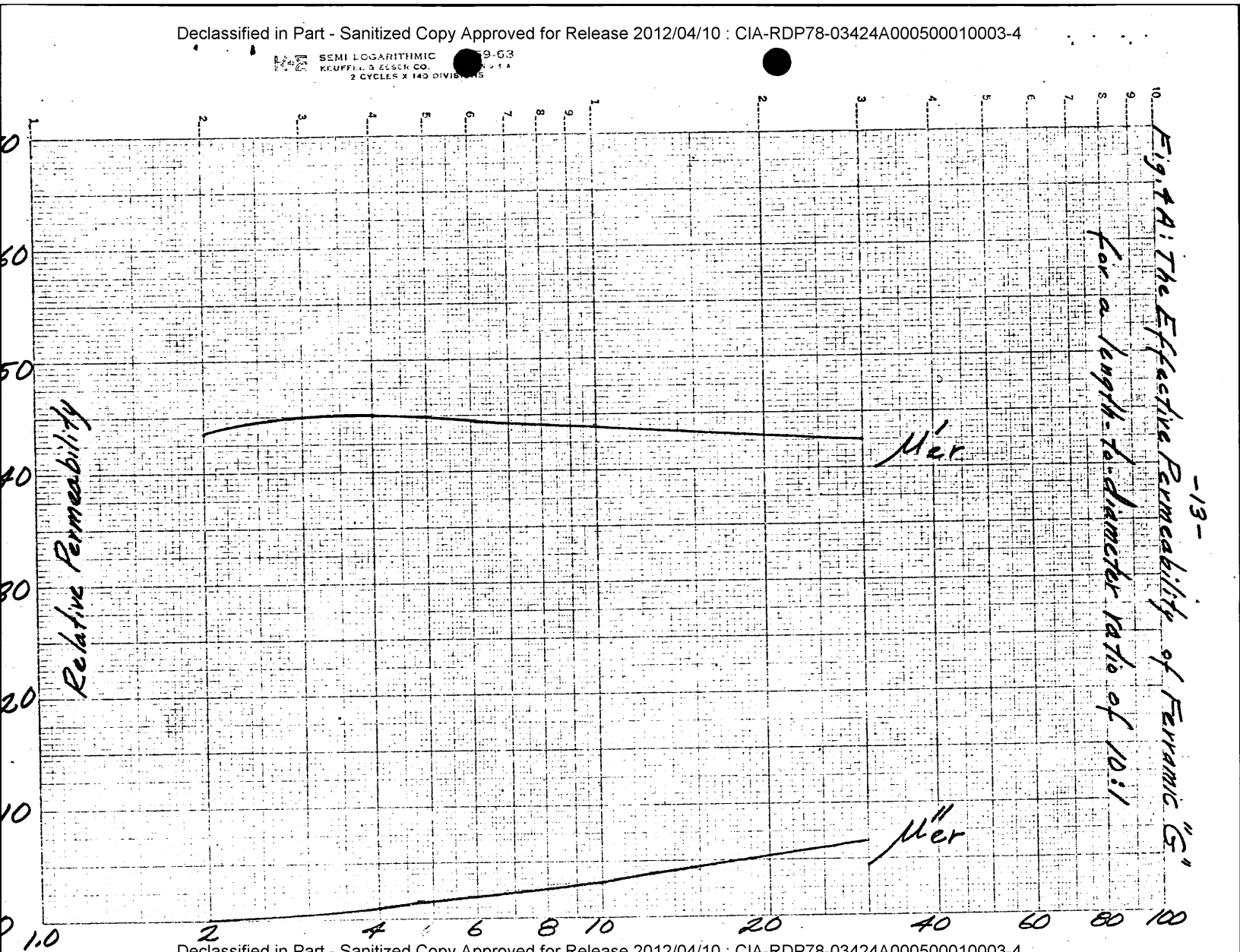

Fig. #4: The Effective Permeability of Ferramic "G" for a length-to-diameter ratio of 10:1

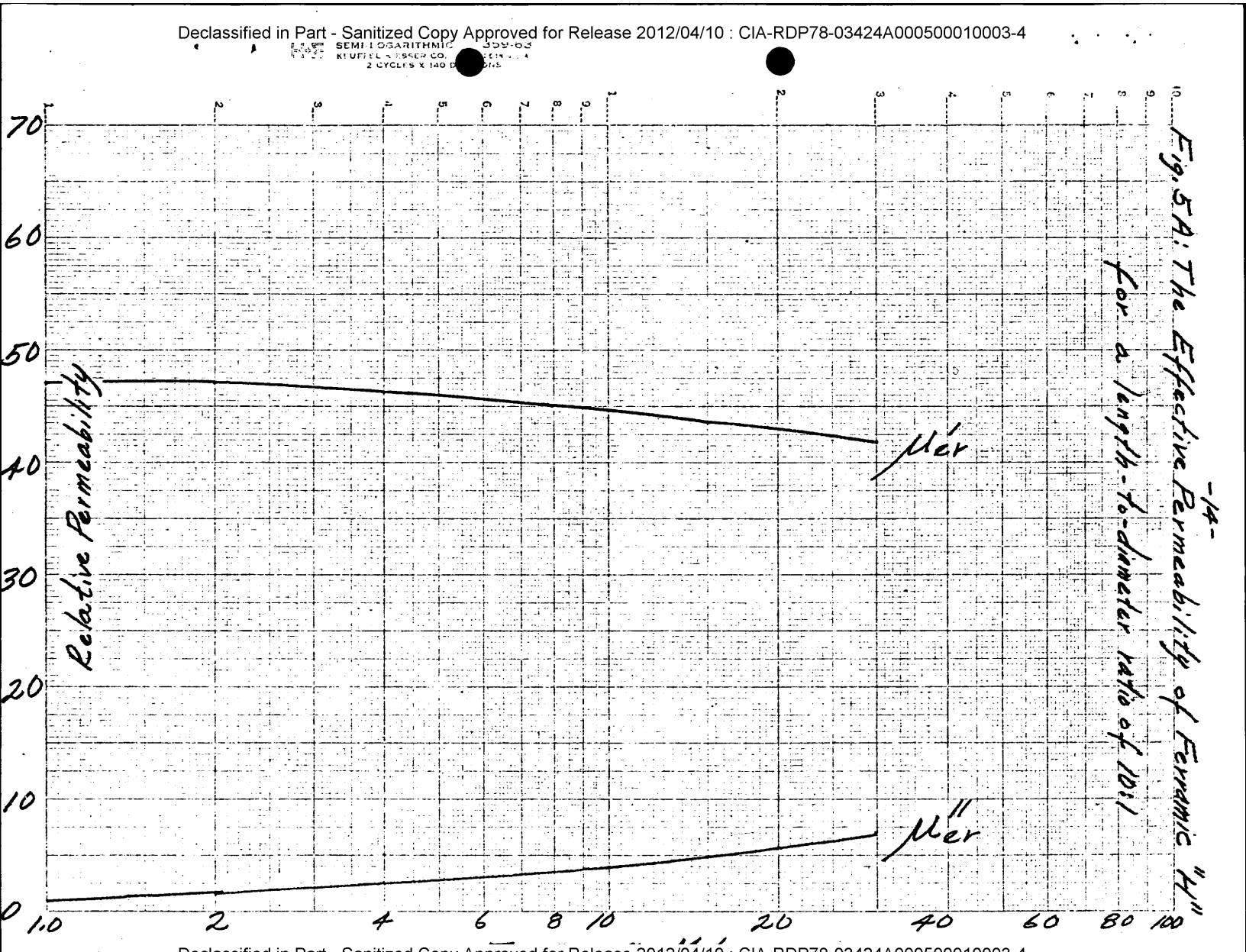

Fig. 5A: The Effective Permeability of Ferramic "H" for a length-to-diameter ratio of 10:1

For needles, the effective permeability approaches the intrinsic permeability. For D = 0:

$$\mu'_{er} = \mu'_{ir}$$
$$\mu''_{er} = \mu''_{ir} \qquad (9)$$

For discs, the effective permeability approaches the permeability of free space. For D = 1:

$$\mu'_{er} = 1$$
$$\mu''_{er} = 0 \qquad (10)$$

Effective permeabilities have been calculated for spheroids made of those materials for which the intrinsic permeabilities have been measured. Figures 3a, 4a, and 5a show the effective permeabilities of these spheroids with a length-to-diameter ratio of 10. Note that the frequency dependence of effective permeability can be quite different from the frequency dependence of intrinsic permeability depending upon the relative values of μ'_i, μ''_i, and D.

B. ANTENNA PERFORMANCE

1. Ferrite Loop Antennas

The effective permeability is a useful parameter for describing the performance of ferrite loop antennas. Consider a loop antenna having a ferrite core the form of a small prolate spheroid and wound with "n" closely spaced conducting turns uniformly spaced along its axis. This configuration closely approximates the usual application and yet is amenable to analysis.

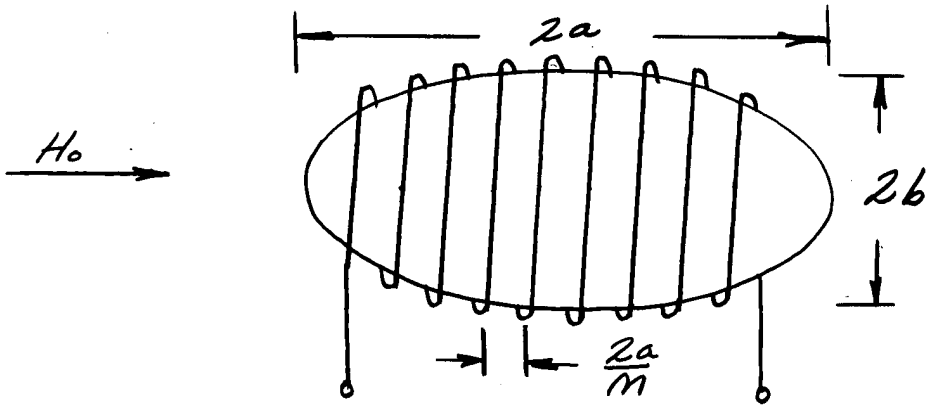

FIGURE 7
FERRITE LOOP ANTENNA

An expression for the voltage induced in the loop antenna by a uniform magnetic field directed along the antenna's axis was derived in the first quarterly report[2].

$$e_i = \left[\omega_o H_o \frac{n}{2a} V\right] \mu_e \tag{11}$$

The volume of the spheroid is

$$V = 4/3\ \pi ab^2 \tag{12}$$

However, now the effective permeability is to be considered complex, causing the induced voltage to be out of phase with the magnetic field. Thus, the magnitude of the induced voltage becomes

$$|e_i| = \left[\omega_o H_o \left(\frac{n}{2a}\right) V\right] \sqrt{\mu_e'^2 + \mu_e''^2} \tag{13}$$

An expression for the antennas input impedance is derived in Appendix D.

$$Z = R + j\,\omega_o L \tag{14}$$

$$R = \left[\omega_o \left(\frac{n}{2a}\right)^2 V (1 - D)\right] \mu_e'' \tag{15}$$

$$L = \left[\left(\frac{n}{2a}\right)^2 V (1 - D)\right] \mu_e' \tag{16}$$

The quality factor of the coil is

$$Q_e = \frac{R}{\omega_o L} = \frac{\mu_e'}{\mu_e''} \tag{17}$$

If the copper losses are included, the quality factor becomes

$$1/Q_{tot} = 1/Q_w + 1/Q_e \tag{18}$$

where

$$Q_w = \frac{\omega_o L}{R_w} \tag{19}$$

and R_w is the high frequency resistance of the wire[3].

$$R_w = \frac{\sqrt{f}}{D} \sqrt{\mu_r \frac{\rho}{\rho_c}} \times 10^{-6} \text{ ohm/ft} \tag{20}$$

ρ = resistivity of conductor at T° C

ρ_c = resistivity of conductor at 20° C

μ_r = relative permeability of conductor

f = frequency in cps

D = diameter of conductor in inches

An equivalent circuit for the ferrite antenna is shown in Figure 8.

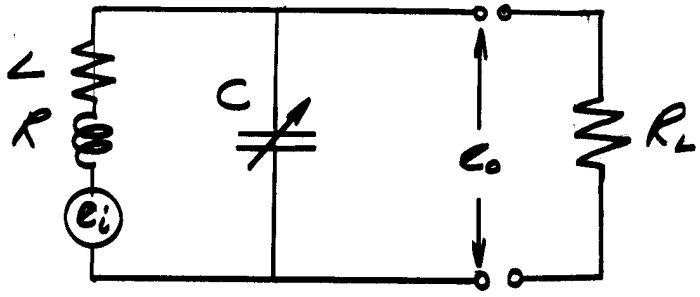

FIGURE 8

EQUIVALENT CIRCUIT OF FERRITE ANTENNA

The induced terminal voltage at resonance is

$$e_o = Q\, e_i \tag{21}$$

where "Q" is the loaded quality factor. If copper losses and loading are negligible

$$e_o = \left[\omega_o H_o \left(\frac{n}{2a}\right)\right] V \quad \frac{\mu_e' \sqrt{\mu_e'^2 + \mu_e''^2}}{\mu_e''} \tag{22}$$

Similarly, the signal-to-noise ratio for the ferrite antenna as developed in the first quarterly report

$$\sigma^2 = \frac{1}{4\, kT \Delta f} \left(\frac{e_i^2\, Q}{L}\right)$$

becomes for complex permeabilities

$$\sigma^2 = \frac{\omega_o H_o^2}{4 kT \Delta f} \left[\frac{V}{(1-D)} \frac{(\mu_e'^2 + \mu_e''^2)}{\mu_e'} Q \right] \tag{23}$$

For negligible copper losses and loading

$$\sigma^2 = \frac{\omega_o H_o^2}{4 kT \Delta f} \left[\frac{V}{(1-D)} \frac{\mu_e'^2 + \mu_e''^2}{\mu_e''} \right] \tag{24}$$

2. Air Core Loop Antennas

Similar expressions describing the performance of an air core loop antenna were developed in the first quarterly report. They are summarized in this section. A sketch of the antenna is shown in Figure 9.

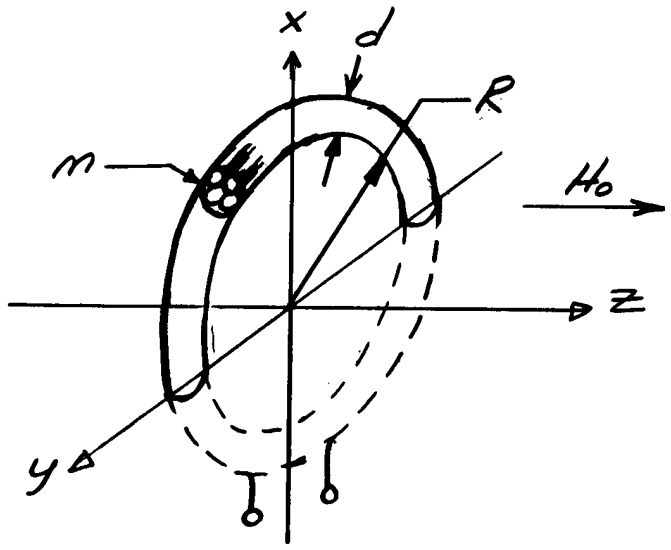

FIGURE 9
AIR CORE LOOP ANTENNA

$$e_i = \omega_o \mu_o H_o n\pi R^2 \tag{25}$$

$$L \approx n^2 \mu_o R \left[\ell n (16 R/d) - 2 \right] \tag{26}$$

$$e_o = Q e_i \tag{27}$$

$$= \frac{\omega_o H_o^2}{4 kT \Delta f} \left[\frac{\mu_o \pi^2 R3 Q}{\ell n (16 R/d) - 2} \right] \tag{28}$$

3. Monopole Antenna

It is instructive to compare the loop antenna with a monopole antenna such as the one shown in Figure 10. The monopole antenna consists of a conducting

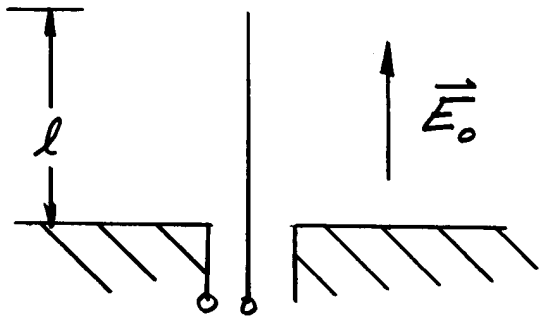

FIGURE 10
MONOPOLE ANTENNA

wire perpendicular to a ground plane. When the antenna is placed in a uniform electric field parallel with the wire, there is a voltage induced along the wire

$$e_i = E_o \ell \tag{29}$$

The monopole can be coupled to a tuned resonant circuit as shown in Figure 11.

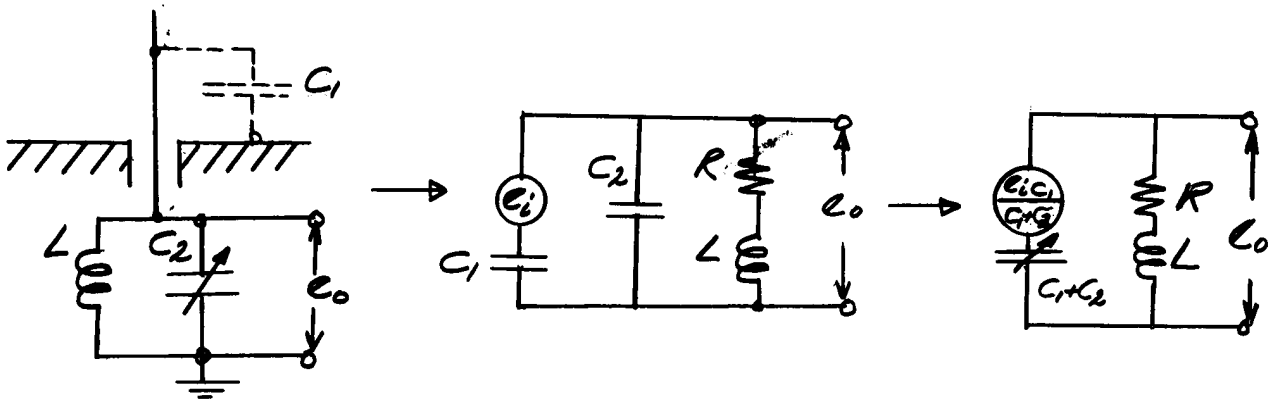

FIGURE 11
MONOPOLE ANTENNA WITH RESONANT CIRCUIT

Two simplified equivalent circuits are also shown. The output voltage is

$$e_o = Q \left(\frac{C_1}{C_1 + C_2} e_i\right) \qquad (30)$$

C. COMPARISON OF ANTENNAS

1. Comparison of Ferrite and Air Core Loop Antennas

The preceding section describes analytically the quasi-static behavior of several antennas. The expressions given therein can also be used to compare the performance of those antennas. However, laboratory measurements are desirable to confirm that this simplified theory adequately describes their performance.

Consider the induced terminal voltage of a ferrite core loop relative to an air core loop. The relative gain is

$$G = 20 \log \frac{\left[Q\, e_i\right]_{MAG}}{\left[Q\, e_i\right]_{AIR}} \text{ db} \qquad (31)$$

$$= 20 \log \frac{\left[n \sqrt{\mu_{er}'^2 - \mu_{er}''^2}\, A\, Q\right]_{MAG}}{\left[n\, A\, Q\right]_{AIR}} \qquad (32)$$

where

A_{MAG} = Cross-sectional area of ferrite rod

A_{AIR} = Area of air core loop

The relative gain is plotted in Figure 12 for the following parameters:

a. Ferrite Loop

n = 5

ℓ = 6" L = 1.56 μh

D = 1/4"

b. Air Core Loop

n = 2

L = 1.54 μh

D = 6-1/4"

These parameters were chosen to result in antennas with approximately equal maximum dimensions and inductances. The ferrite rod was approximated by its inscribed

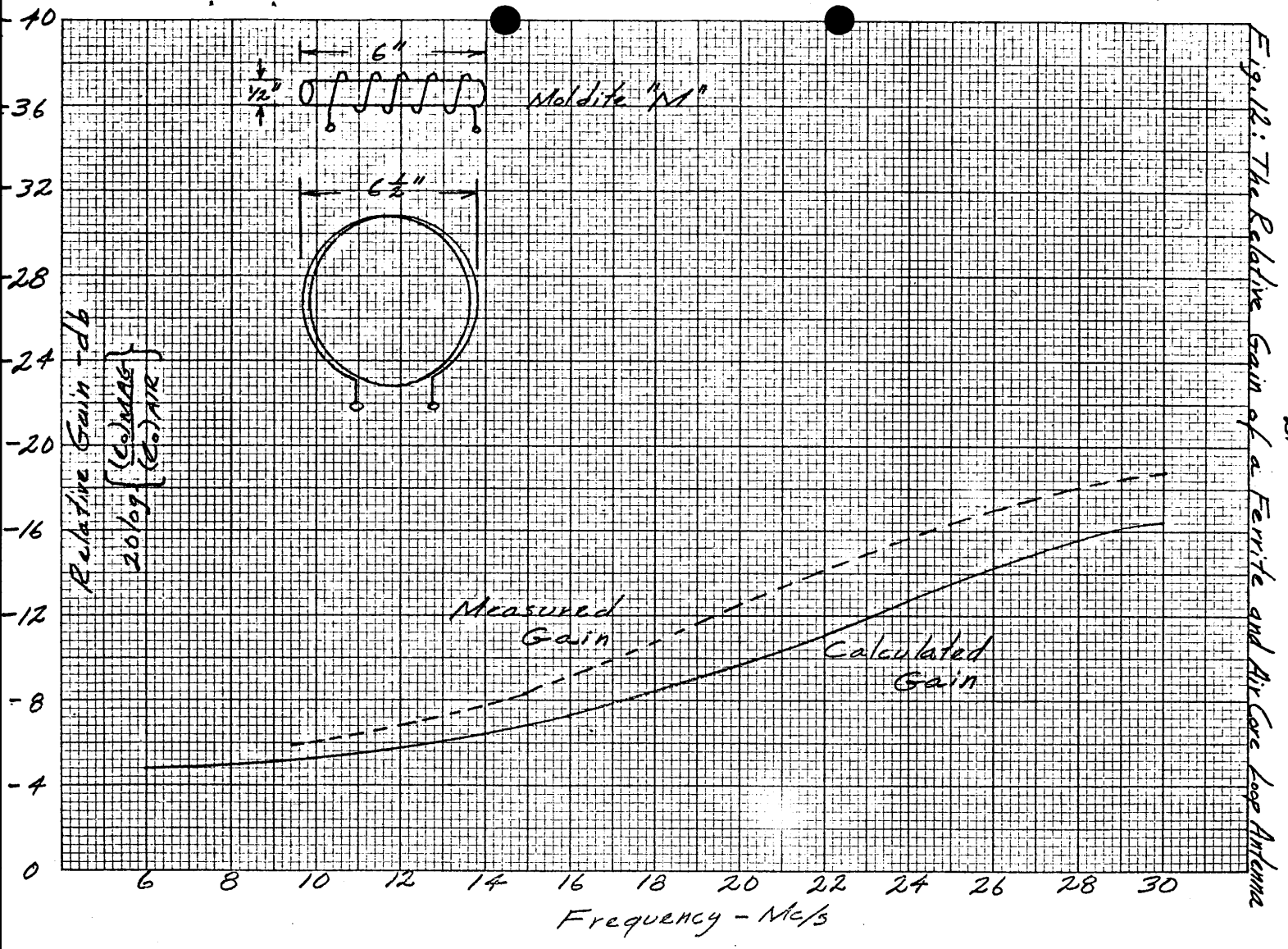

Fig. 12: The Relative Gain of a Ferrite and Air Core Loop Antenna

prolate spheroid. The real part, imaginary part, and modulus of the effective permeability are plotted in Figure 13.

The loaded "Q" was measured with a Boonton 260-A "Q" Meter rather than calculated. Since a low impedance receiver was used to measure the gain, an impedance matching transformer was required. The loaded "Q" was, therefore, characterized by the antenna, transformer, and receiver impedances and was not conveniently calculated. However, it was shown that the theory adequately describes the coil inductance and core losses. For example, the unloaded "Q" of the antenna was calculated using equations 16 - 20 and then compared with the measured values of unloaded "Q". See Figure 14.

The relative gain of the ferrite and air core loops was also measured and compared with the calculated values in Figure 12. The measurements were conducted inside an RF screen room using an Empire Devices NF105 Field Intensity Meter. The violation of certain assumptions are probably responsible for the slight displacement of the measured performance from the calculated performance. For example, the five turns on the ferrite rod were not closely space, the core was a cylinder and not a spheroid, and the antennas were in the induction not the radiation fields. However, the simplified theory is considered to give an excellent qualitative description of the antenna and a sufficiently accurate quantitative description for most design purposes.

The gain of the ferrite antenna is approximately 5 db down from the gain of the air core antenna below 10 mc/s. The degraded performance of the ferrite antenna above 10 mc/s is attributed to increased core losses. Note the behavior of μ''_{er} in Figure 13.

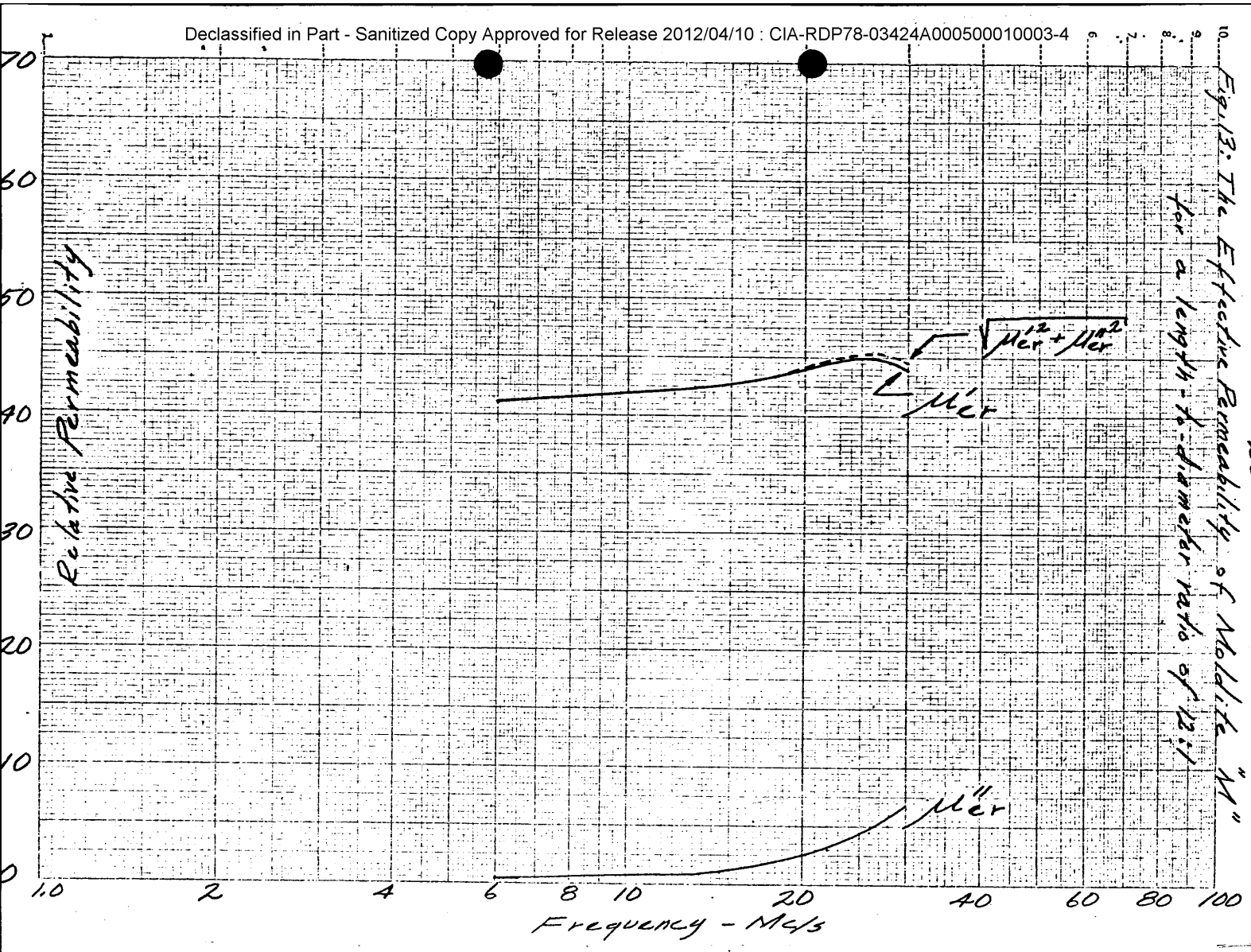

Fig. 13: The Effective Permeability of Molalite "M" for a length - to - diameter ratio of 12:1

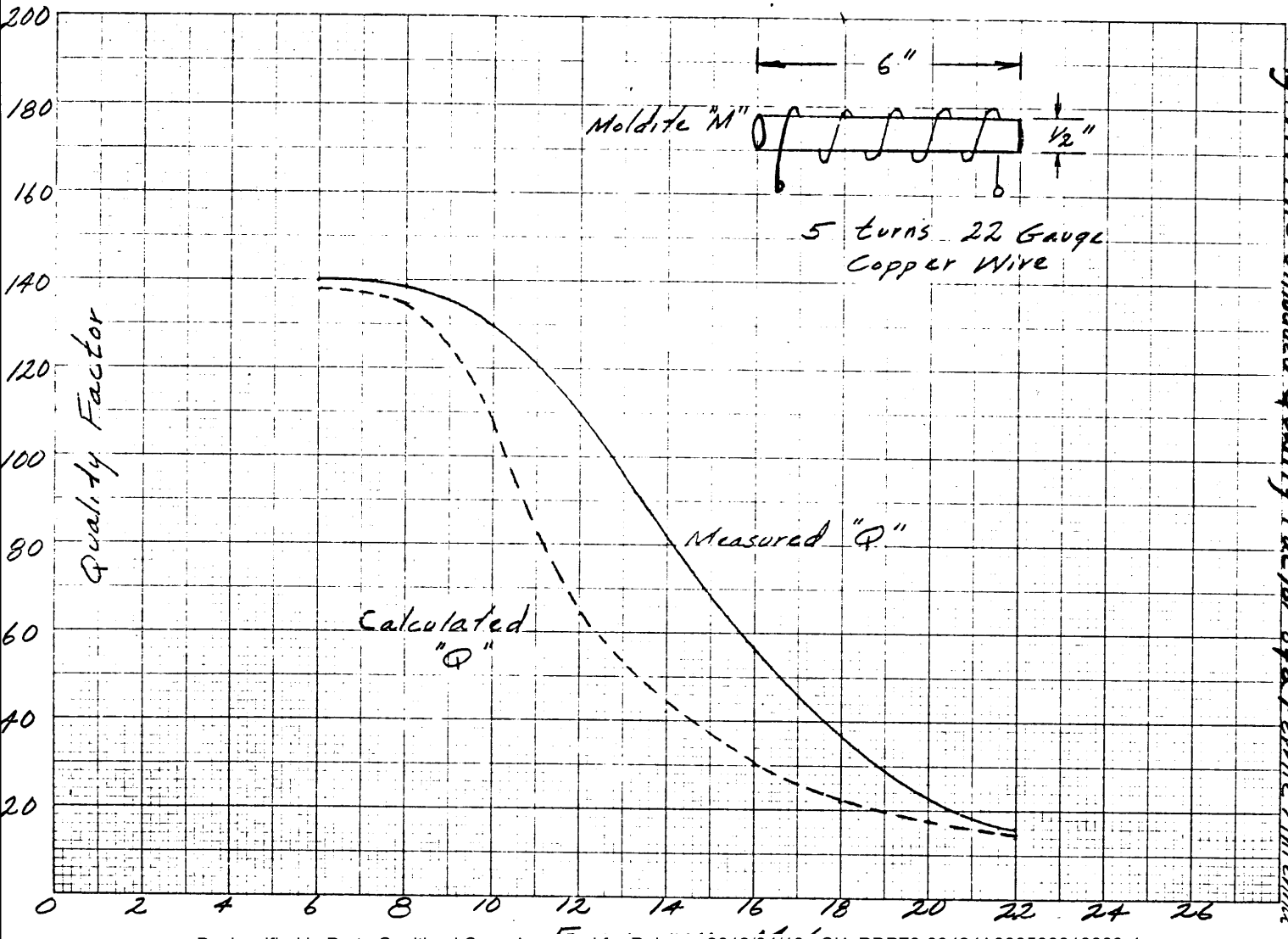

Fig. 14: The Unloaded Quality Factor of a Ferrite Antenna

2. Comparison of Monopole and Loop Antennas

The monopole antenna is used extensively, being simple and inexpensive to manufacture, of a convenient geometry, and easily stowed. We can compare the performance of the monopole with the ferrite antenna directly, but it is more instructive to compare the performance of the monopole with a simple loop. The basic differences between the loop and open wire configurations are thereby more easily discerned. Then, the comparison of performance between the ferrite and monopole antenna can be inferred, using previous results.

The loop antenna can be considered coupled to the electric field or to the magnetic field with equal validity. Refer to Appendix E. To compare the loop and monopole antennas most clearly, consider them both coupled to the electric field. The two antennas are shown in Figure 15.

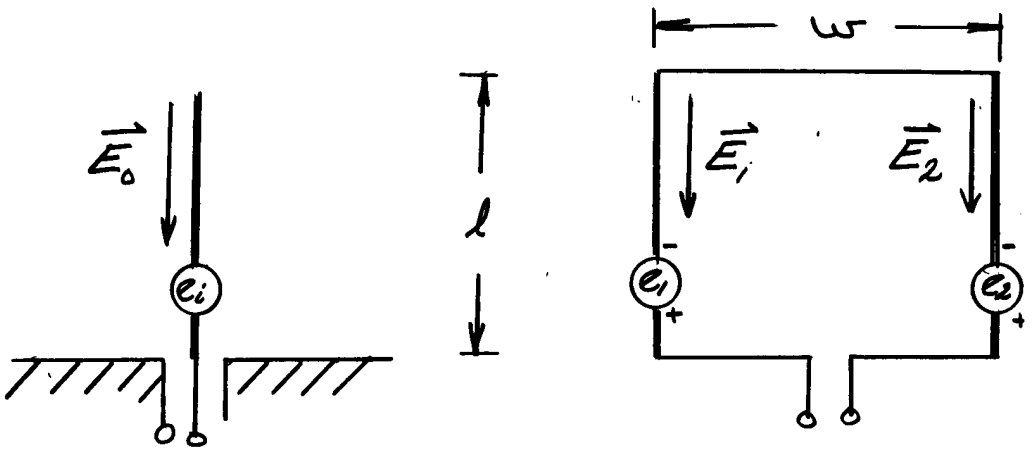

a. - Monopole Antenna

b. - Loop Antenna

FIGURE 15

COMPARISON OF MONOPOLE AND LOOP ANTENNAS

The voltage induced in the monopole antenna is

$$e_m = E_o \ell \tag{33}$$

The loop antenna is equivalent to two displaced monopole antennas connected in series, phase opposed. The voltage induced in the loop is the difference between the voltages induced in each of the two equivalent monopoles

$$\begin{aligned} e_L &= e_1 - e_2 \\ &= E_1 \ell - E_2 \ell \end{aligned} \tag{34}$$

The two voltages nearly cancel for small antennas, differing in the far field only by the phase delay incurred by the electric field as the energy propagates across the width of the loop. Therefore, the voltage induced in a small loop is considerably less than the voltage induced in a monopole of comparable size. For larger antennas where the width of the loop becomes equal to a half wavelength, the voltages induced in the two legs add rather than cancel, and the loop voltage becomes twice the monopole voltage. An expression for the gain of the loop antenna relative to the monopole antenna on an induced voltage basis can be derived using equations (29) and (E-4)

$$\Delta G\,(e_i) = 20 \log \left\{ \frac{2\left[\ell \sin\left(\frac{\pi w}{\lambda}\right)\right]_{\text{loop}}}{[\ell]_{\text{monopole}}} \right\} \quad \text{db} \tag{35}$$

$$\approx 20 \log \left\{ \frac{2\pi}{\lambda} \frac{[\ell w]_{\text{loop}}}{[\ell]_{\text{monopole}}} \right\} \quad \text{db} \qquad , w \ll \lambda$$

The relative gain is plotted in Figure 16 for the case

$$\ell = w = 6.25 \text{ inches}$$

At this point, the monopole, by virtue of its greater induced voltage, appears to have an advantage over the loop as a small antenna. However, it is less difficult to couple the loop into a tuned resonant circuit. In fact, the loop antenna forms the inductive element of the tuned circuit.

3 cyc. x 170 1mm Divisions

25X1

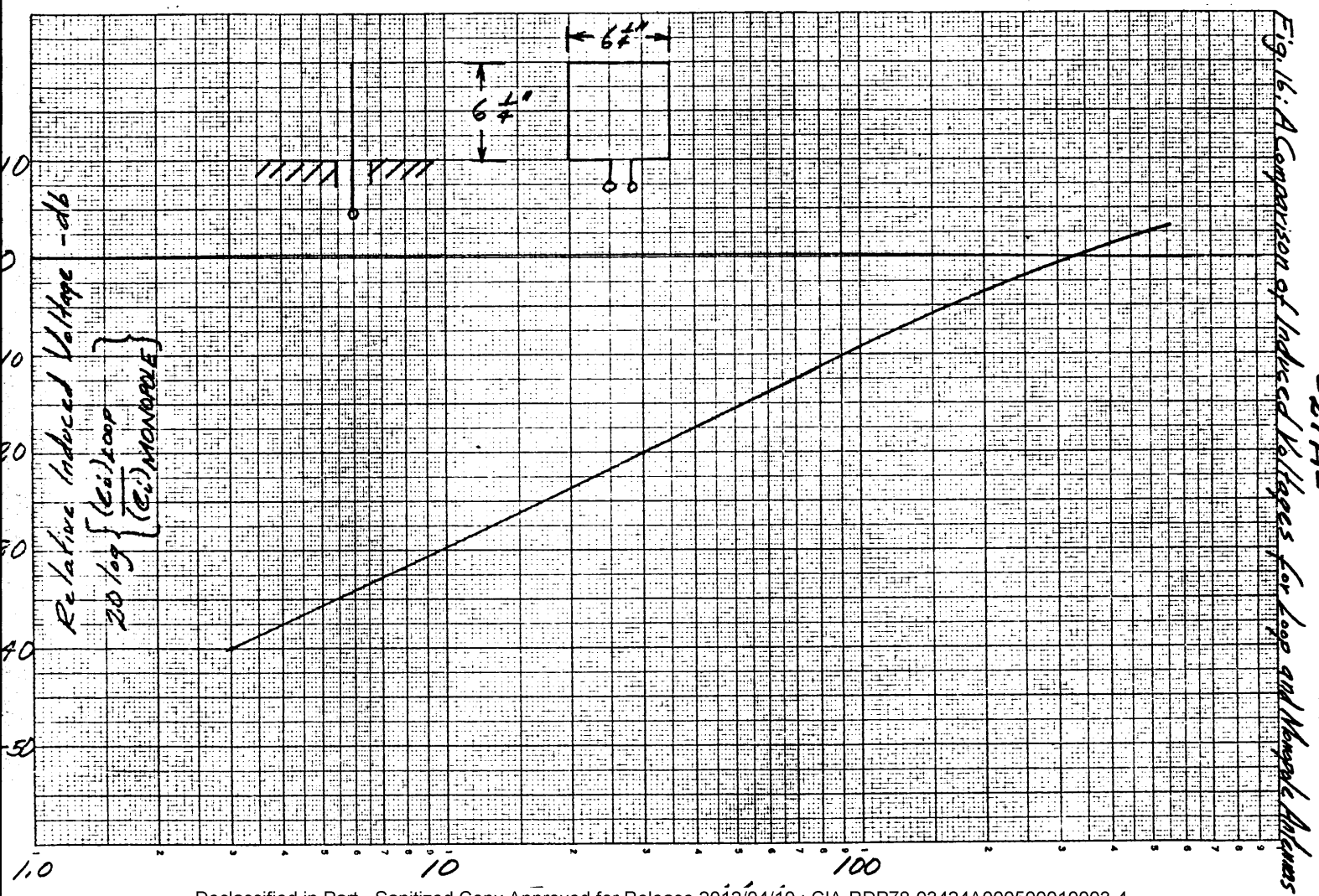

Fig. 16: A Comparison of Induced Voltages for Loop and Monopole Antennas

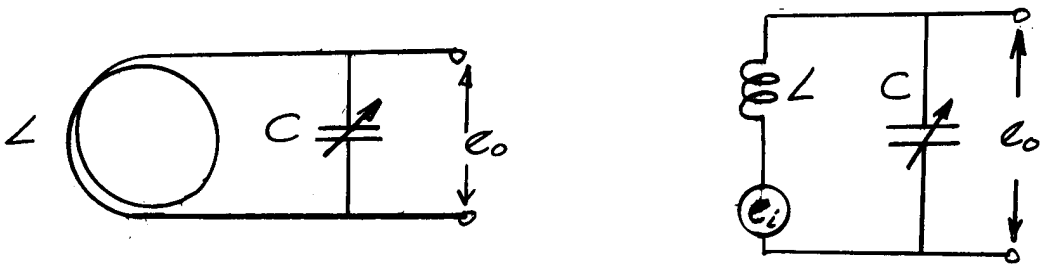

a. - Antenna and Resonant Circuit b. - Equivalent Circuit

FIGURE 17

THE LOOP ANTENNA AND RESONANT CIRCUIT

It has already been shown that, when a monopole is coupled into a resonant circuit in a conventional manner, the induced voltage is effectively reduced by a factor $(c_1)/(c_1 + c_2)$. Refer to Equation (30) and the accompanying discussion. To keep the resonant circuit tuned

$$c_1 + c_2 = 1/\omega_0^2 L \qquad (36)$$

Therefore, assuming c_1 is constant, the effective induced voltage for the monopole decreases 40 db/decade as the frequency is reduced.

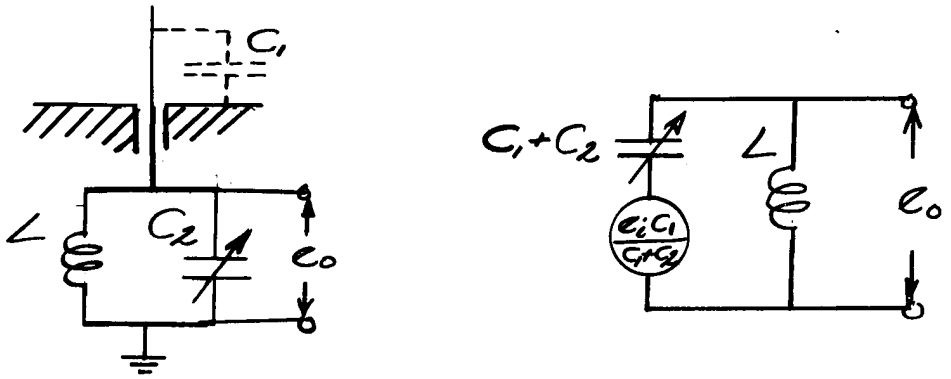

a. Antenna and Resonant Circuit b. - Equivalent Circuit

FIGURE 18

THE MONOPOLE ANTENNA AND RESONANT CIRCUIT

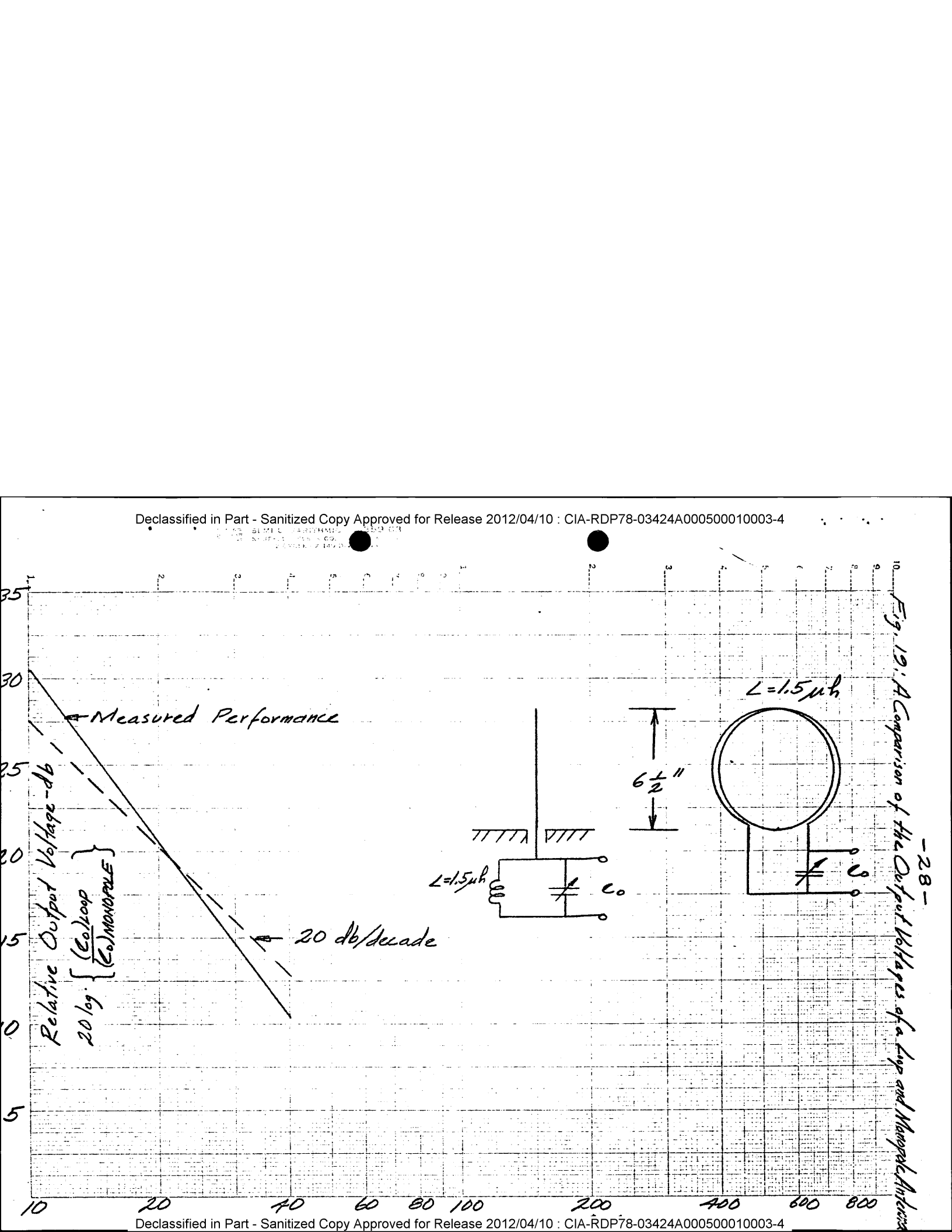

Fig. 12: A Comparison of the Output Voltages of a Loop and Monopole Antenna

Now a complete comparison can be made between the output voltages of the loop and monopole antennas. Summarizing, the induced voltage in the monopole increases over the induced voltage in the loop 20 db/decade as the frequency is lowered. However, the monopole suffers approximately a 40 db/decade loss in the coupling network. Therefore, for equal "Q" circuits, the output voltage for the monopole can be expected to decrease relative to the loop 20 db/decade. This behavior is illustrated in Figure 19 where the measured performance of a monopole antenna relative to a loop antenna is presented graphically. Although the voltage induced per turn in the loop decreases 20 db/decade with frequency, the number of turns in the loop can be increased when the antenna is designed for a lower operating frequency. For a fixed range in tuning capacitance, the required number of turns is inversely proportional to the center frequency exactly compensating for the reduced voltage per turn. The net voltage remains nearly constant for a change in operating frequency for the loop as it does for the monopole.

D. DISPERSION EFFECTS

1. Introduction

Recall that the permeability of ferrite is frequency dependent. The real part of the complex permeability decreases with frequency. It has already been shown that the inductance of a coil wound on a ferrite core is proportional to the real part of the permeability. Therefore, it should be possible to make an inductance which also decreases with frequency.

A frequency dependent inductance can produce "automatic tuning" of a parallel resonant circuit. Consider the resonant LRC circuit shown in Figure 20. The resonant frequency is

$$\omega_o = \frac{1}{\sqrt{LC}} \qquad (37)$$

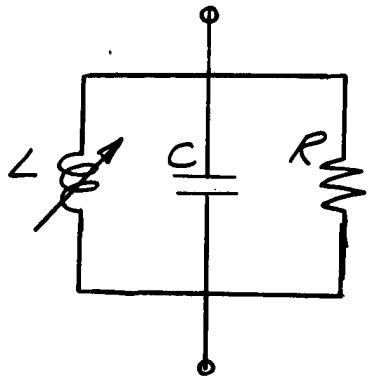

FIGURE 20
PARALLEL RESONANT CIRCUIT WITH FREQUENCY
DEPENDENT INDUCTANCE

Suppose that it were possible to form an inductance decreasing as the reciprocal of the frequency squared.

$$L = \frac{\left(\frac{1}{C}\right)}{\omega^2} \tag{38}$$

Then the resonant frequency would exactly track the operating frequency

$$\omega_o \equiv \omega \tag{39}$$

The circuit would remain tuned, and its impedance bandwidth would be infinite

$$\Delta f \rightarrow \infty \tag{40}$$

If the inductance decreased as $1/\omega$ instead of $1/\omega^2$, the bandwidth would become

$$\Delta f = 1/\pi RC \tag{41}$$

whereas, for constant inductance, it would be

$$\Delta f_o = 1/2\pi RC \tag{42*}$$

These expressions are derived in Appendix F. The results are summarized in Figure 21.

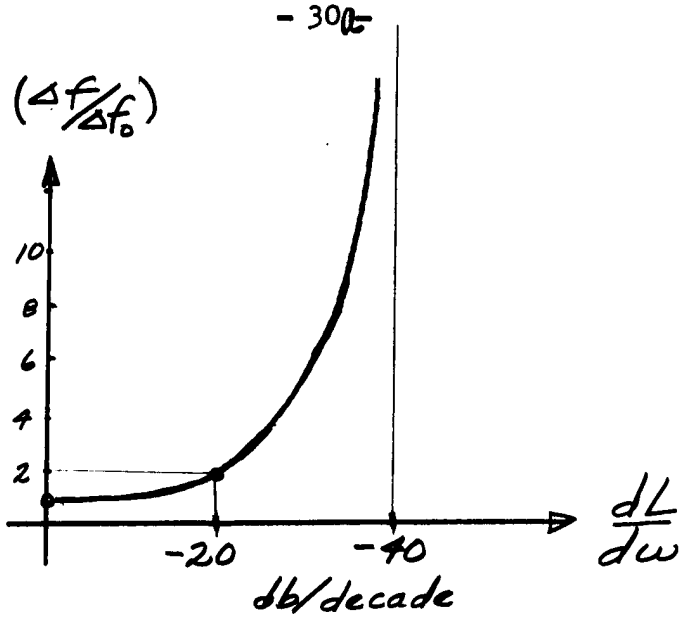

FIGURE 21
IMPROVED BANDWIDTH ACHIEVED WITH FREQUENCY DEPENDENT INDUCTANCE

Note that the greatest improvement in bandwidth occurs when the inductance falls off faster than 20 db/decade.

2. Dispersive Antenna Coupling Network

Now consider the monopole antenna with the coupling network shown in Figure 22. Let the inductance be formed by a toroidal coil with a dispersive core. Then the impedance Z_2, Figure 22, displays an increased bandwidth compared

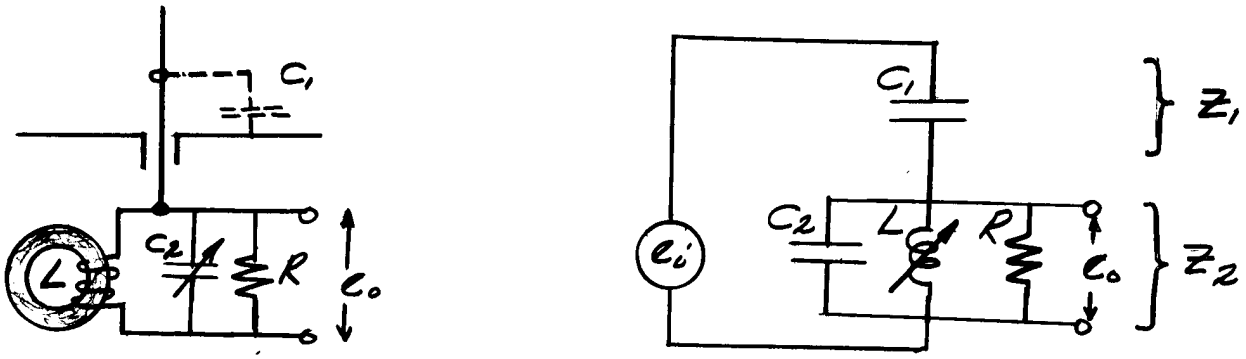

FIGURE 22
MONOPOLE ANTENNA WITH DISPERSIVE COUPLING NETWORK

to the case of an equal inductance with a non-dispersive core. The output voltage is

$$e_o = \left(\frac{Z_2}{Z_1 + Z_2}\right) e_i \qquad (43)$$

$$\approx \left(\frac{Z_2}{Z_1}\right) e_i \quad , \quad Z_1 \gg Z_2$$

It is predominantly Z_2 which determines the output voltage bandwidth. See Figure 23. Therefore, the output voltage exhibits approximately the same improvement in bandwidth by the introduction of the dispersive core as does the impedance Z_2.

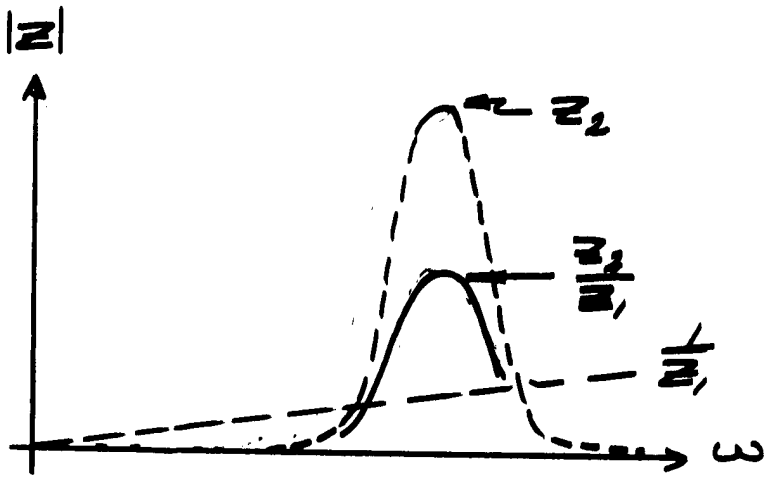

FIGURE 23

In actual practice, we were unable to achieve any advantage using dispersive media in the coupling network. The losses were extremely large. The quality factor for the toroidal coil was less than two in the region of dispersion. These results are consistent with the permeability measurements reported in Figures 4 and 5. Not only are the losses high, they are also frequency dependent which acts to decrease the impedance bandwidth. Furthermore, even in the absence of losses, the decrease in real permeability was less than 20 db/decade and would be ineffective for producing significantly increased bandwidths.

Thus, the dispersive core material is responsible for the coupling network's poor performance. The losses are too large and the dispersion too small. No suitable material was found reported in the literature. Furthermore, there is theoretical evidence that the desired characteristics are not physically realizable[6,7,8].

3. A Loop Antenna with a Dispersive Core

Next consider the possibility of using ferrite core material to an advantage in the ferrite loop antenna. The performance of this antenna was described in Section IV-B. The results developed there will be used here without further reference.

The equivalent circuit for the antenna is shown in Figure 24. To keep the antenna tuned by dispersion, the inductance and, consequently, the real part of the effective permeability must decrease as the reciprocal of the frequency squared.

$$\mu_e' \propto 1/f^2 \qquad (44)$$

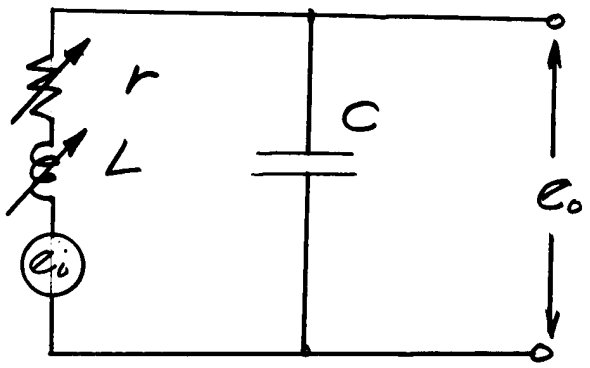

FIGURE 24
THE EQUIVALENT CIRCUIT OF THE FERRITE LOOP ANTENNA WITH A DISPERSIVE CORE

The output voltage is

$$e_o = Q\, e_i \qquad (45)$$

For negligible cooper losses, the quality factor is

$$Q = \frac{\mu_e'}{\mu_e''} \tag{46}$$

The induced voltage is proportional to the effective permeability

$$e_i \propto \sqrt{\mu_e'^2 + \mu_e''^2} \tag{47}$$

For broadband operation, the output voltage must be constant. Therefore,

$$\left(\frac{\mu_e'}{\mu_e''}\right) \sqrt{\mu_e'^2 + \mu_e''^2} = K \tag{48}$$

For the high Q case

$$\frac{\mu_e'}{\mu_e''} \sqrt{\mu_e'^2 + \mu_e''^2} \approx \frac{\mu_e'^2}{\mu_e''} \tag{49}$$

Therefore, broadband operation requires that

$$\frac{\mu_e'^2}{\mu''_e} = K \tag{50}$$

But since

$$\mu_e' \propto 1/f^2 ,$$

it is necessary that

$$\mu_e'' \propto 1/f^4$$

It appears hopeless to specify a 20 db/decade decrease in the real part of the effective permeability simultaneously with a 40 db/decade decrease in the imaginary part over a wide range in frequencies. No combination of material and geometry was found to even approximate the desired behavior of the effective permeability. Also, experimental results did not indicate any significant improvement in bandwidth by using dispersive core materials in ferrite loop antennas.

4. A Theoretical Relationship Between Losses and the Dispersion of Real Permeability

No significant advantages were found using dispersive materials in small antennas. The dispersion by real permeability was too weak and the accompanying losses too great in all available materials to be of any advantage. Furthermore, a theoretical treatment of the problem indicates that the desired behavior over a wide band of frequencies is not physically realizable.

The permeability is a complex function of frequency

$$\mu = \mu'(\omega) - j\mu''(\omega)$$

There is, in general, an interdependence between the real and imaginary parts of a complex function. If, for example, the function exhibits a certain requisite analytic behavior, the interdependence can be expressed by the Hilbert transform integral. J. S. Toll has proven that the complex permeability consists of such a Hilbert Transform pair[8]. The prescribed analytic behavior is equivalent to a finite upper bound on the signal velocity. No signal can be transmitted with a velocity greater than the velocity of light, Consequently,

$$\mu_r'(\omega_o) = 1 + 2/\pi \int_0^\infty \frac{\omega\, \mu_r''(\omega)}{\omega^2 - \omega_o^2}\, d\omega \qquad (52)$$

and

$$\mu_r''(\omega_o) = -\frac{2\omega_o}{\pi} \int_0^\infty \frac{[\mu_r''(\omega) - 1]}{\omega^2 - \omega_o^2}\, d\omega$$

The Cauchy principal value of the integrals are to be taken. Note that, if the frequency behavior of the real permeability is everywhere specified, the losses are completely determined.

The interdependence of the real and imaginary parts of the complex permeability can also be described in terms of the modulus of the complex permeability

$$|\mu_r| = \sqrt{\mu_r'^2 + \mu_r''^2} \qquad (53)$$

and the quality factor of the material

$$Q = \mu_r'/\mu_r'' \qquad (54)$$

Bode derived the expression(9)

$$Q(\omega_o) = \cot an \left\{ \frac{\pi}{2} \left| \frac{dA}{dx} \right|_{\omega_o} + 1/\pi \int_{-\infty}^{+\infty} \left[\left| \frac{dA}{dx} \right|_{\omega} - \left| \frac{dA}{dx} \right|_{\omega_o} \right] \ell n \coth \left| \frac{x}{2} \right| dx \right. \qquad (55)$$

where

$$A = \ell n \left| \mu_r \right|$$

$$x = \ell n \, \omega/\omega_o$$

$$\left| \frac{dA}{dx} \right| = 1/20 \quad db/dec$$

It should be noted, however, that there is not a unique loss associated with any prescribed amplitude behavior. Equation (55) gives the minimum loss that can occur consistent with a prescribed frequency dependence of the modulus of complex permeability. Since losses were prohibitive in the region of dispersion, the minimum loss case is of greatest interest.

Graphical solutions to Bode's equations have been developed which have facilitated this analysis(10). Figures 25 and 26 show a graphical solution. In Figure 25, the complex permeability was assumed to be

$$\mu_r = 200 \left(\frac{1 + j\omega/210}{1 + j\,\omega/18} \right) \qquad (56)$$

Both the amplitude of the relative permeability and the corresponding minimum loss tangent are shown. Note that the amplitude exhibits a 20 db/dec attenuation over a 10:1 frequency band. There is a corresponding 20 db/dec dispersion in the real part of the equivalent complex permeability. See Figure 25. Note that the losses increase substantially before the real permeability decreases significantly, the greatest losses occur in the region of maximum dispersion, and the quality factor decreases to less than unity in the dispersive region. Compare these results with the measured behavior of complex permeability in Figures 3, 4, and 5. Clearly, recent theory suffices to explain the qualitative behavior of complex permeability. Furthermore, the theory places severe fundamental limitations on the dispersive behavior of ferrites. There appears little chance of developing improved materials to better utilize dispersive effects to an advantage.

25X1

4 Log Cycles × 90 Divisions

Fig. 25: The Amplitude of Effective Permeability and Its Minimum Loss Angle

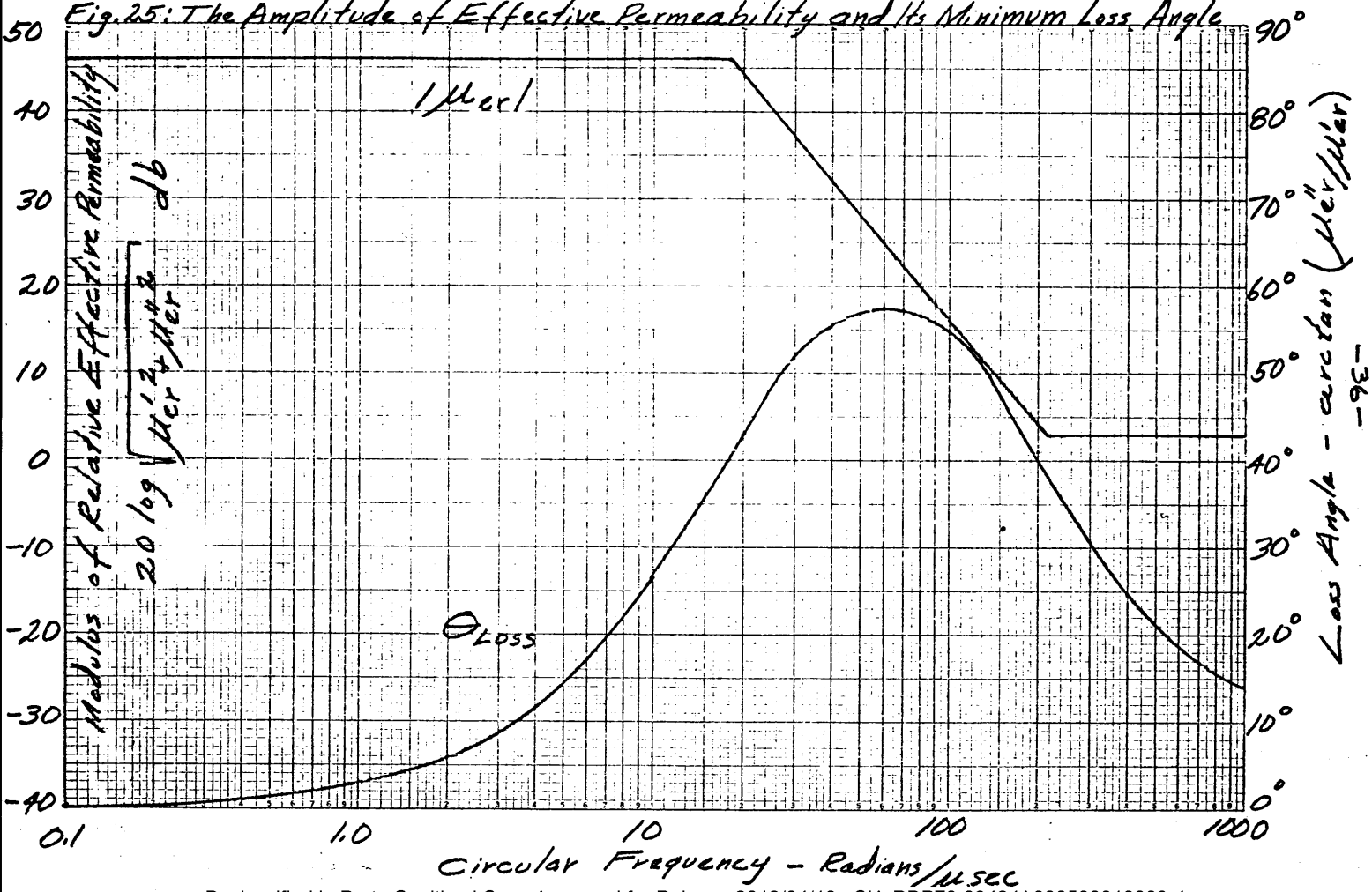

4 Log Cycles × 90 Divisions

25X1

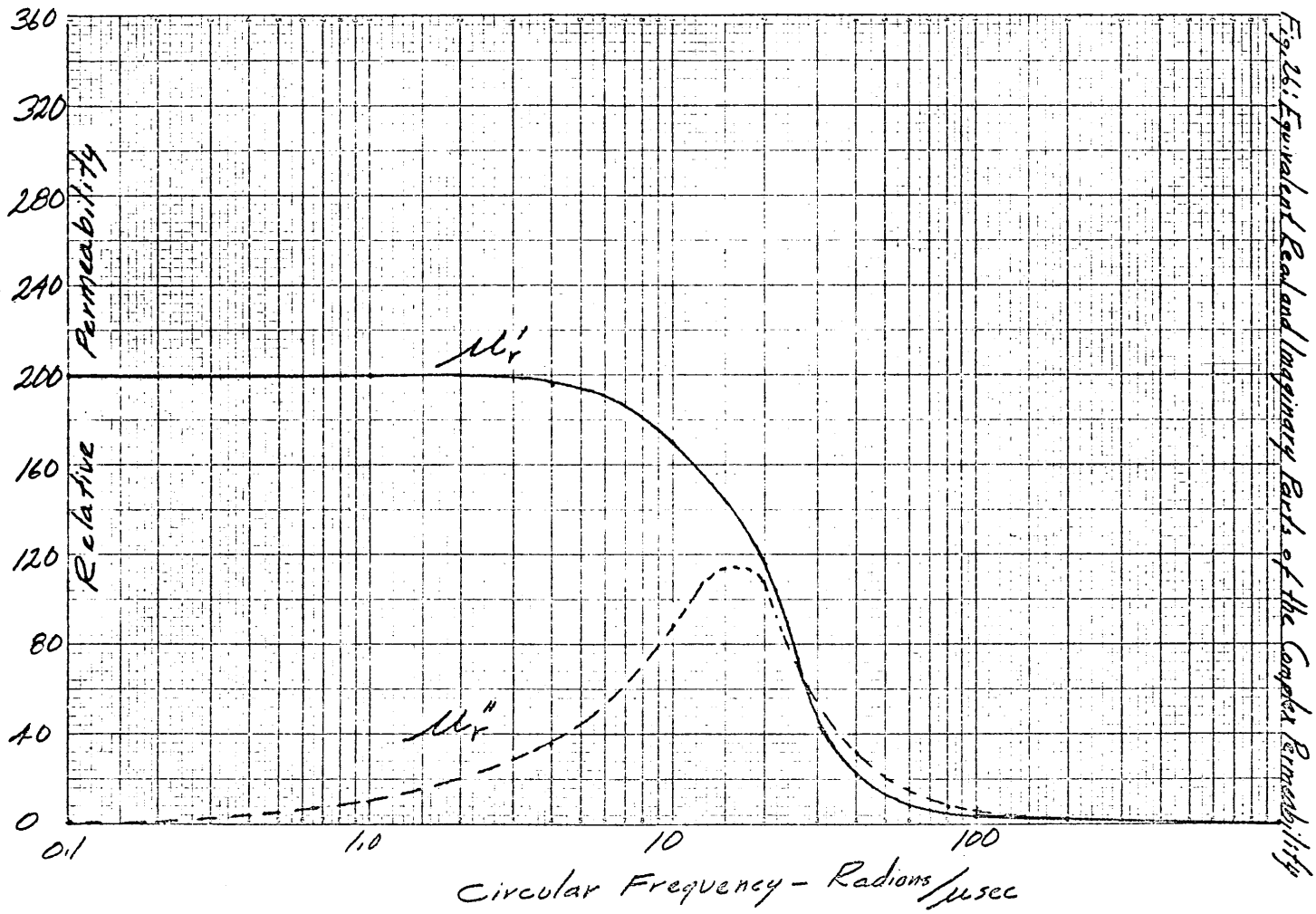

Fig. 26: Equivalent Real and Imaginary Parts of the Complex Permeability

E. THEORETICAL PERFORMANCE OF SMALL ANTENNAS

Without dispersive effects, the theoretical limitations on physically small antennas developed by Chu appear quite imposing[11]. Chu showed that the maximum gain-bandwidth product of an omnidirectional antenna is limited by its physical size. The gain of a small, lossless antenna designed for a maximum gain-bandwidth product was found to nearly equal the gain of a half-wave dipole, but its bandwidth became vanishingly small. The bandwidth can be increased by loading the antenna, but the gain of the antenna is thereby decreased. Suppose that an antenna were of optimum design, providing a gain-bandwidth product equal to the theoretical maximum derived by Chu, and were then loaded to achieve additional bandwidth. An expression was derived in the first quarterly report for the loss in gain produced by loading the optimum antenna in order to achieve a prescribed bandwidth.

$$\Delta G = -20 \log \left[\frac{\Delta f}{2 f_o} \left(\frac{\lambda}{2\pi a} \right)^3 \right] \quad \text{db} \qquad (57)$$

where

ΔG = loss in gain

Δf = prescribed bandwidth

$2a$ = maximum dimension of the antenna

λ = free space wavelength at center frequency

f_o = center frequency

The expression is valid for antennas with a maximum dimension much less than a wavelength and producing either an electric or a magnetic dipole-like radiation field.

Figures 27 and 28 show two applications of Equation (57). Consider an antenna 6-1/4" long. Let a normalized bandwidth of 1/2% be required. Figure 27 shows the loss in gain that will result as a function of center frequency when the specified bandwidth is achieved by loading Chu's optimum antenna. At low frequencies, the size of the antenna measured in wavelengths becomes smaller. Consequently, the inherent bandwidth becomes smaller. Thus, greater loading will be required and higher losses will result as the operating frequency is reduced.

Next consider an antenna designed to operate at a center frequency of 10 mc/s with a normalized bandwidth of 1/2%. Figure 28 shows the gain of the loaded optimum antenna as a function of antenna length. Note that a 60 db loss in gain can be expected if the antenna size is to be reduced by a factor of 10.

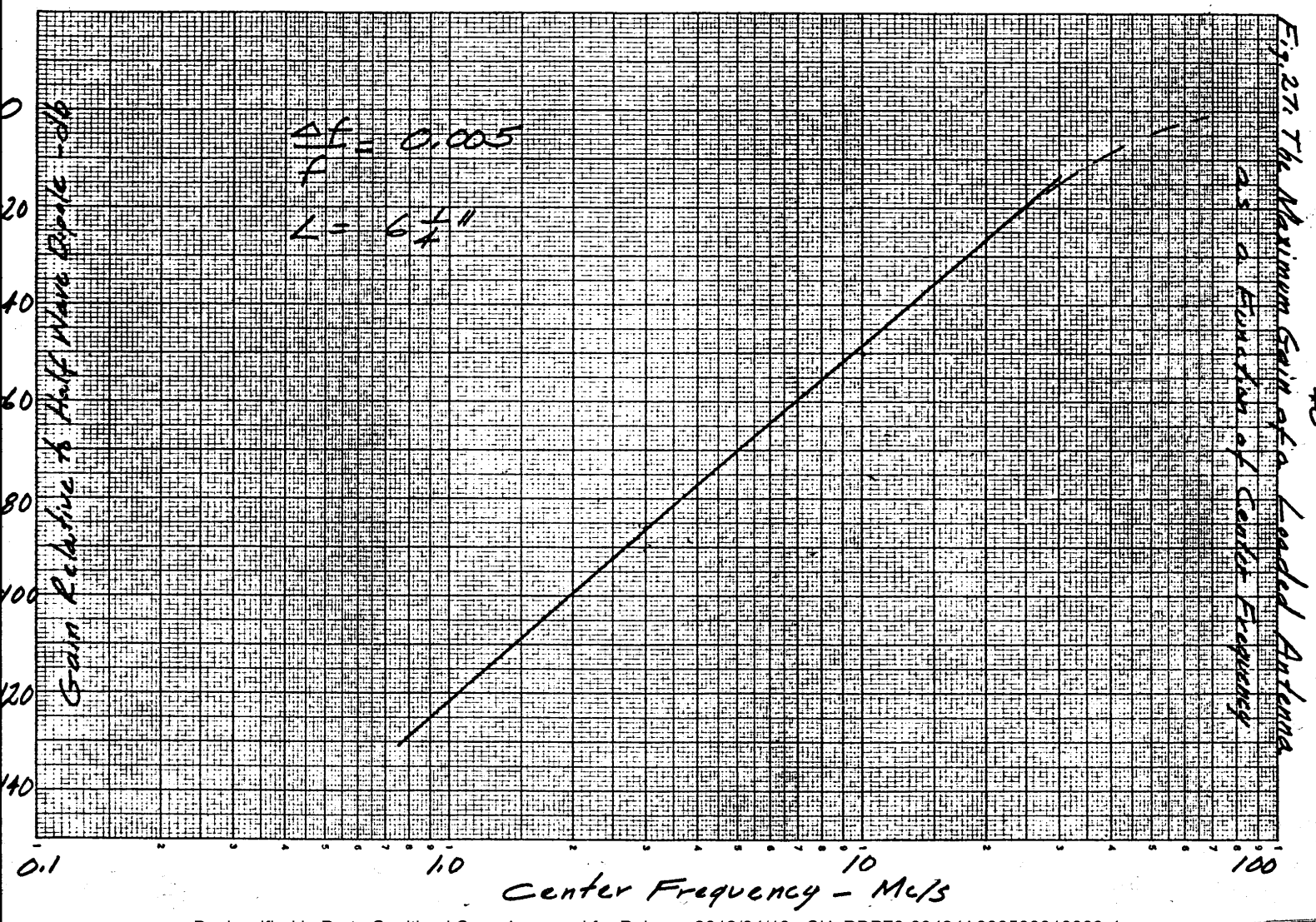

Fig. 27. The Maximum Gain of a Loaded Antenna as a Function of Center Frequency

40

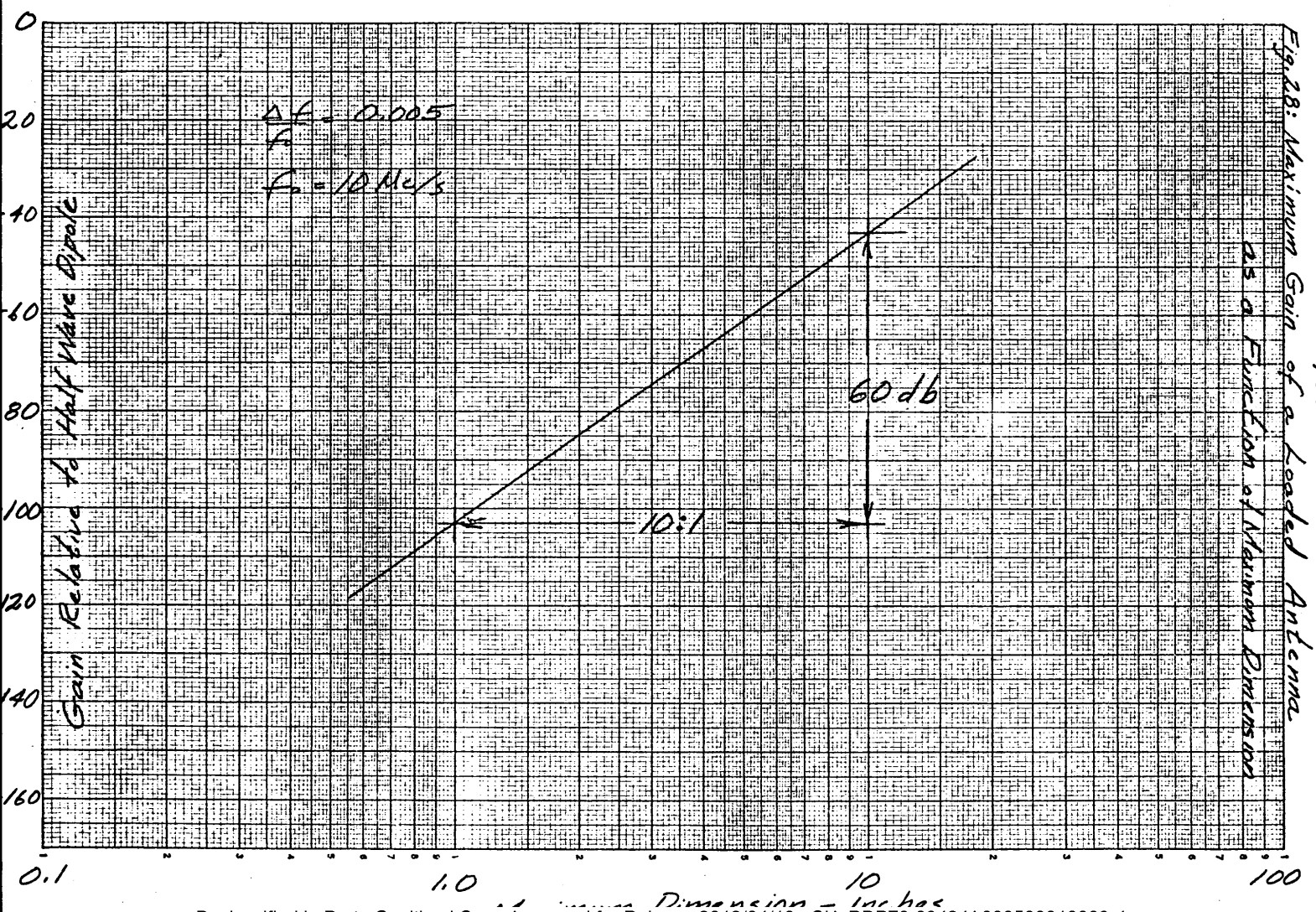

Fig. 28: Maximum Gain of a Loaded Antenna as a Function of Maximum Dimension

V. REFERENCES AND BIBLIOGRAPHY

A. REFERENCES

1. "Demagnetization Factors of the General Ellipsoid", J. A. Osborn, Phys. Rev. Number 67, June 1945.
2. [redacted] 25X1
3. Reference Data for Radio Engineers, 4th Edition, International Telephone and Telegraph Corporation, 1956.
4. Principles of Electricity and Electromagnetism, G. P. Hornwell, McGraw-Hill.
5. "Inductive Aerials in Modern Broadcast Receivers", H. Blok and J. Rietveld, Philips Technical Review, Vol. 16, No. 7, Jan. 1955.
6. "Realizability of a Prescribed Frequency Variation of Dielectric Constant", R. J. Harrison, Proc. IRE, Vol. 45, No. 3, March 1957.
7. "Dispersion Relations for Tensor Media and their Application to Ferrites", B. S. Gourary, J.A.P. Vol. 28, No. 3, March 1957.
8. "Causality and the Dispersion Relation: Logical Foundation", J. S. Toll, Phys. Rev., Vol. 104, No. 6, Dec. 15, 1956.
9. Network Analysis and Feedback Amplifier Design, H. W. Bode, D. Van Nostrand Co., Inc., N.Y., N.Y. 1945.
10. Servomechanism and Regulating System Design, Chestnut and Mayer, John Wiley and Sons, Inc., N.Y. 1951.
11. "Physical Limitations of Omnidirectional Antennas", Journal of Applied Physics, Vol. 19, No. 12, Dec. 1948.

B. BIBLIOGRAPHY

1. "Improving Ferrite Cored Antennas", C. A. Grimmett, Tele-Tech and Electronic Industries, Vol. 14, No. 2, Feb. 1955.
2. Input Impedance of a Spherical Ferrite Antenna with a Latitudinal Current, W. L. Weeks, Tech. Report No. 6, Antenna Laboratory, University of Illinois, Aug. 1955.
3. Impedance of Ferrite Loop Antennas, V. H. Rumsey and W. L. Weeks, Tech. Report No. 13, Antenna Laboratory, University of Illinois, Oct. 1956.
4. "Inductive Aerials in Modern Broadcast Receivers", H. Blok and J. J. Rietveld, Philips Technical Review, Vol. 16, No. 7, Jan. 1955.
5. "A Magnetic Radio Compass Antenna Having Zero Drag", A. A. Hemphill, IRE Transactions - Aeronautical and Navigational Electronics, ANE-2, No. 4, Dec. 1955.

6. "The Magnetic Antenna", L. Page, Phys. Rev.Vol. 69, No. 11, 12, June 1946.

7. Ferromagnetic Loop Aerials for Kilometric Waves, J. S. Belrose, Wireless Engineer, Feb. 1955.

8. [redacted] 25X1

VI. NOMENCLATURE

μ_i - intrinsic permeability

μ_e - effective permeability

μ_r - relative permeability

μ_o - permeability of free space

μ' - real part of complex permeability

μ'' - imaginary part of complex permeability

$|\mu|$ - modulus of complex permeability

$\vec{B}$ - magnetic flux density

$\vec{H}$ - magnetic field intensity

$\vec{E}$ - Electric field intensity

D - demagnetization factor

e_i - induced voltage

e_o - output voltage

e - eccentricity of prolate spheroid

V - volume of prolate spheroid

Q - quality factor

R - resistance

L - inductance

C - capacitance

ω - circular frequency

f - frequency

Δf - 3 db bandwidth

ΔG - relative gain

k - Boltzmann's constant

T - absolute temperature

σ^2 - signal-to-noise ratio

APPENDIX A

ELLIPTICAL HYSTERESIS LOOP

The equation which defines permeability is

$$\bar{B} = \mu_i \bar{H} \tag{A-1}$$

Consider sinusoidal time variations and a complex permeability

$$\bar{H} = \bar{H}_o \, e^{j\omega t} \tag{A-2}$$

$$\mu_i = \mu_i' - j\,\mu_i''$$

Then

$$\bar{B} = \bar{H}_o (\mu_i' \cos \omega t + \mu_i'' \sin \omega t) + j\,\bar{H}_o (\mu_i' \sin \omega t - \mu_i'' \cos \omega t) \tag{A-3}$$

The physical observables are

$$\mathrm{Re}[\bar{H}] = (\bar{H}_o) \cos \omega t$$
$$\mathrm{Re}[\bar{B}] = (H_o \sqrt{\mu_i'^2 + \mu_i''^2}) \sin (\omega t + \gamma) \tag{A-4}$$

where $\tan \gamma = \dfrac{\mu_i'}{\mu_i''}$

It can be seen that these expressions define an elliptical hysteresis loop by considering the equation for an ellipse expressed in terms of its eccentric anomaly "ϕ".

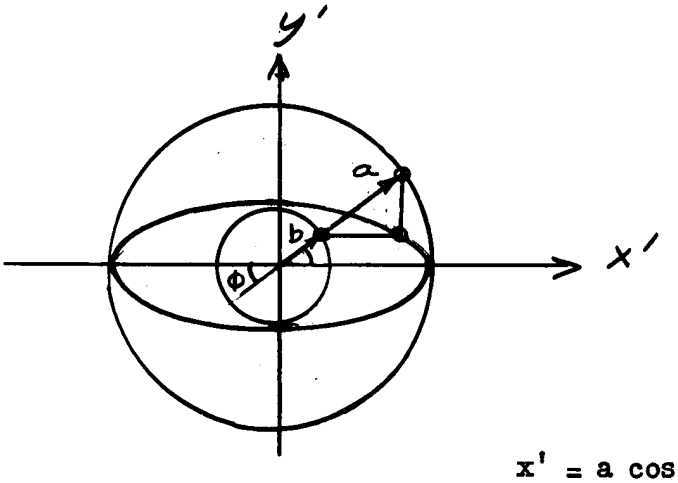

$$x' = a \cos \phi$$
$$y' = b \sin \phi \tag{A-5}$$

FIGURE A-1

Consider a rotation of coordinate axes

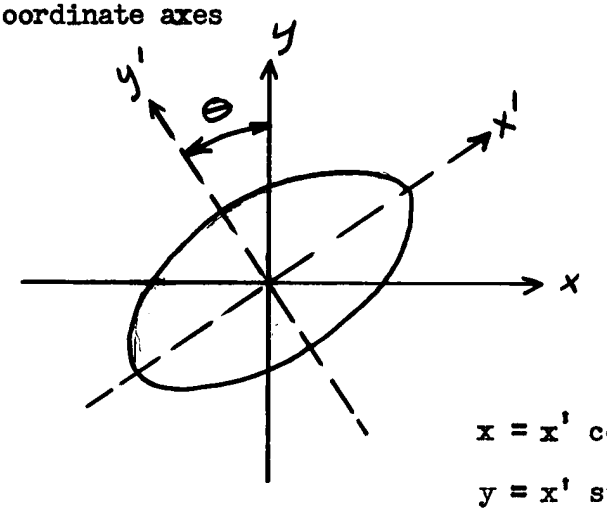

$$x = x' \cos\theta - y' \sin\theta$$
$$y = x' \sin\theta + y' \cos\theta \qquad \text{(A-6)}$$

FIGURE A-2

The equations for the ellipse in the new coordinate system become

$$X = (a\cos\theta)\cos\phi - (b\sin\theta)\sin\phi \qquad \text{(A-7)}$$
$$= \sqrt{b^2 + (a^2 - b^2)\cos^2\theta}\ \cos(\phi + \alpha)$$

and

$$y = (a\sin\theta)\cos\phi + (b\cos\theta)\sin\phi \qquad \text{(A-8)}$$
$$= \sqrt{a^2 - (a^2 - b^2)\cos^2\theta}\ \sin(\phi + \beta)$$

where

$$\tan\alpha = (b/a)\tan\theta \qquad \text{(A-9)}$$
and
$$\tan\beta = (a/b)\tan\theta$$

Let

$$H_o = \sqrt{b^2 + (a^2 - b^2)\cos^2\theta}$$
$$H_o\sqrt{\mu_i'^2 + \mu_i''^2} = \sqrt{a^2 - (a^2 - b^2)\cos^2\theta} \qquad \text{(A-10)}$$
$$\omega t = (\phi + \alpha)$$
$$\gamma = (\beta - \alpha)$$

Then the equations for the ellipse become

$$x = H_o\cos\omega t$$
$$y = H_o\sqrt{\mu_i'^2 + \mu_i''^2}\ \sin(\omega t + \gamma) \qquad \text{(A-11)}$$

which are identical with the equations describing the physical observables Re $[\bar{B}]$ and Re $[\bar{H}]$. Therefore, the hysteresis loop is an ellipse.

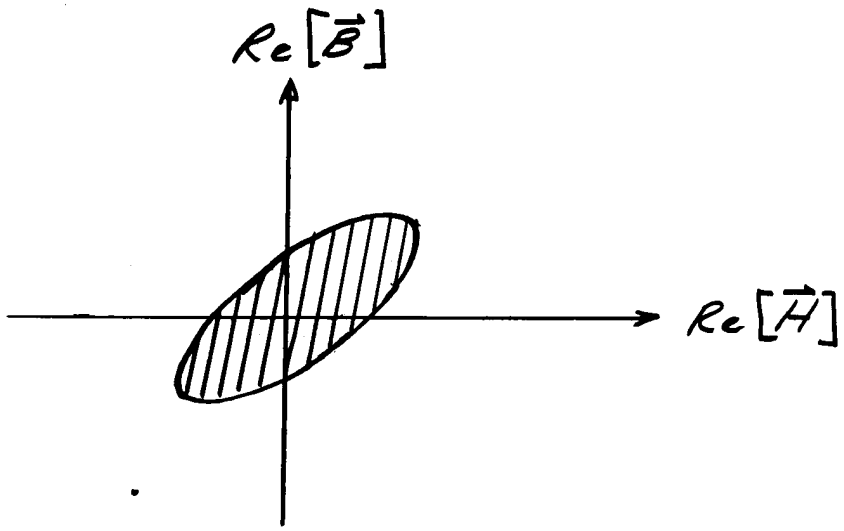

FIGURE A-3

APPENDIX B

COAXIAL MEASUREMENTS OF COMPLEX PERMEABILITY

Consider the input impedance a coaxial waveguide whose electrical length is much less than one wavelength. Let the guide be terminated in a short circuit with a concentric cylinder of ferrite partially filling the guide next to the termination.

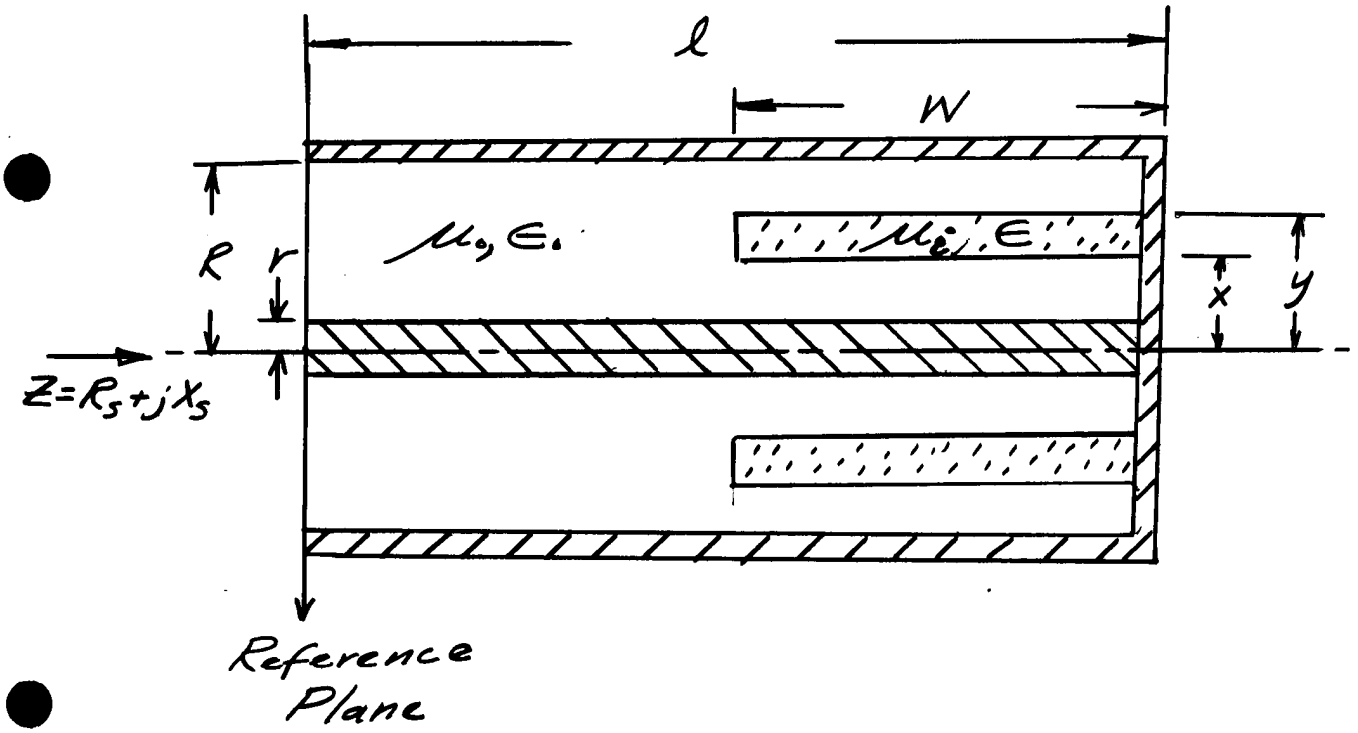

FIGURE B-1

Approximate the magnetic field intensity by the quasi-static solution

$$\bar{H} \approx \frac{I}{2\pi r} e^{j\omega t} \vec{\phi}_i \qquad \text{(B-1)}$$

The voltage induced across the waveguide at the reference is

$$V = d\phi/dt \qquad \text{(B-2)}$$

where

$$\phi = \int_{\text{Longitudinal Half Area}} \mu_i \cdot \bar{H} \cdot d\bar{A} \qquad \text{(B-3)}$$

For the assumed conditions

$$V = j\omega\left[(\ell-W)\int_r^R \mu_o \frac{I}{2\pi r}\,dr + W\int_r^x \mu_o \frac{I}{2\pi r}\,dr + W\int_y^R \mu_o \frac{I}{2\pi r}\,dr + W\int_x^y \mu_i \frac{I}{2\pi r}\,dr\right] \tag{B-4}$$

$$= j\frac{\omega\mu_o}{2\pi} I\left[(\ell-W)\,\ell n\, R/r + W\,(\ell n\, x/r + \ell n\, R/y + \mu_{ir}\ell n\, y/x)\right]$$

where

$$\mu_i = \omega_o\,\mu_{ir} \tag{B-5}$$

Now let

$$\mu_{ir} = \mu_{ir}' - j\,\mu_{ir}'' \tag{B-6}$$

Then

$$V = j\frac{\omega\mu_o I}{2\pi}\left[\ell\,\ell n\, R/r + W\left\{\ell n\, x/r\; R/y\; r/R + (\mu_{ir}' - j\,\mu_{ir}'')\,\ell n\, y/x\right\}\right] \tag{B-7}$$

The input impedance is

$$Z = V/I \tag{B-8}$$

$$= \left[\mu_{ir}''\,\frac{\omega\mu_o}{2\pi}\,(W\,\ell n\, y/x)\right] + j\left[(\mu_{ir}' - 1)\,\frac{\omega\mu_o}{2\pi}\,(W\,\ell n\, y/x) + Z_c\,\frac{\omega\ell}{C}\right]$$

where

$Z_c \triangleq$ characteristic impedance of empty coaxial waveguide

$$= 1/2\pi\sqrt{\frac{\mu_o}{\varepsilon_o}}\;\ell n\, R/r \tag{B-9}$$

and

$C \triangleq$ velocity of light in a vacuum

$$= \frac{1}{\sqrt{\mu_o\,\varepsilon_o}}$$

Therefore, the series impedance

$$Z = R_s + j\,X_s$$

becomes

$$R_s = \mu_{ir}''\left[f\,\mu_o\,(W\,\ell n\, y/x)\right] \tag{B-10}$$

$$X_s = (\mu_{ir}' - 1)\left[f\,\mu_o\,(W\ell n\, y/x)\right] + Z_c\,\frac{\omega\ell}{C} \tag{B-11}$$

Solving for the complex permeabilities

$$\mu''_{ir} = \frac{R_s}{f\,\mu_o\,(W\,\ell n\,y/x)} \tag{B-12}$$

$$\mu'_{ir} = \mu''_{ir}\,\frac{X_s}{R_s} - \frac{Z_c}{Z_o}\,\frac{2\pi\ell}{W\,\ell n\,y/x} + 1 \tag{B-13}$$

where

$$Z_o = \sqrt{\mu_o/\varepsilon_o} \tag{B-14}$$

APPENDIX C

TOROIDAL MEASUREMENTS OF COMPLEX PERMEABILITIES

Consider the input impedance of a toroidal coil wound on a ferrite core of rectangular cross-section. Let all dimensions be small compared to a wavelength.

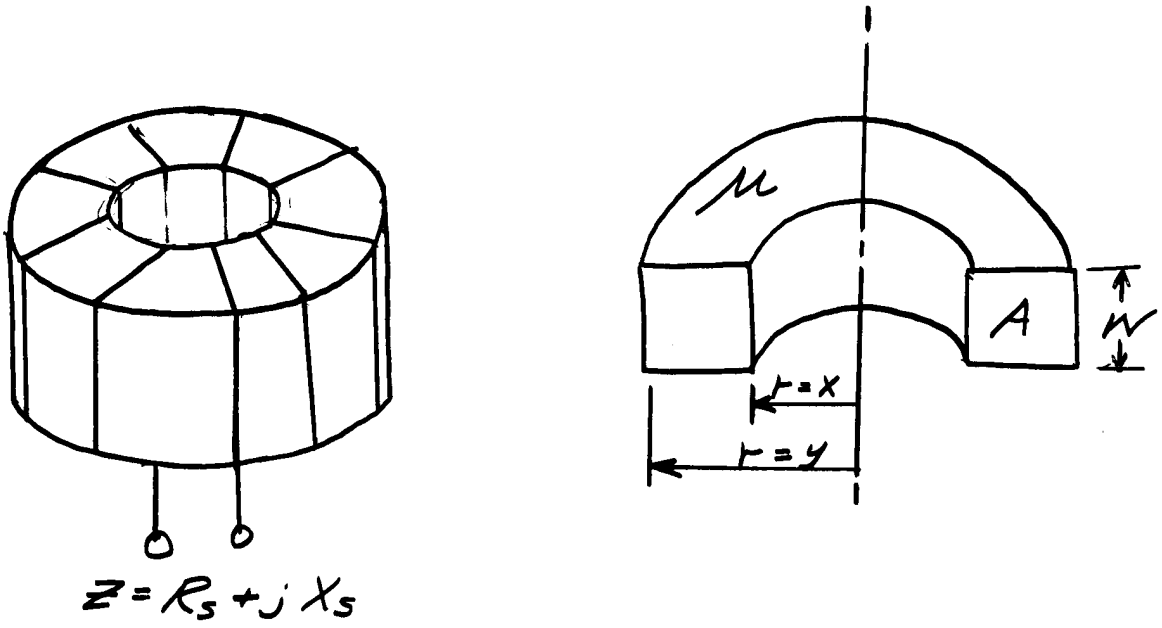

FIGURE C-1

Approximate the magnetic field intensity by the quasi-static solution

$$\bar{H} = \frac{NI}{2\pi r} \; e^{j\omega t} \qquad \text{(C-1)}$$

The induced voltage is

$$V = N \; d\phi/dt = j \omega \mu_i N \int_A \bar{H} \cdot d\bar{A} \qquad \text{(C-2)}$$

$$V = j\omega \mu_i \frac{N^2 I}{2\pi} \int_x^y 1/r \; W dr$$

$$= j\omega \frac{\mu_i N^2 I}{2\pi} W \ln y/x \qquad \text{(C-3)}$$

The input impedance is

$$Z = V/I = R_s + j X_s \qquad (C-4)$$

Let $$\mu_i = \mu_o \ (\mu'_{ir} - j \mu''_{ir}) \qquad (C-5)$$

Then

$$R_s = N^2 f \mu_o \mu''_{ir} \left[W \ell n \, y/x \right] \qquad (C-6)$$

and

$$X_s = N^2 f \mu_o \mu'_{ir} \left[W \ell n \, y/x \right] \qquad (C-7)$$

Solving for the complex permeability

$$\mu''_{ir} = \frac{R_s}{f \mu_o N^2} \left[\frac{1}{W \ell n \, y/x} \right] \qquad (C-8)$$

$$\mu'_{ir} = \mu''_{ir} \frac{X_s}{R_s} \qquad (C-9)$$

APPENDIX D

THE IMPEDANCE OF A COIL WOUND ON A FERROMAGNETIC PROLATE SPHEROID

Consider a prolate spheroid of ferrite material wound with "n" closely spaced conducting turns uniformly spaced along its axis. Analysis shows[4] that,

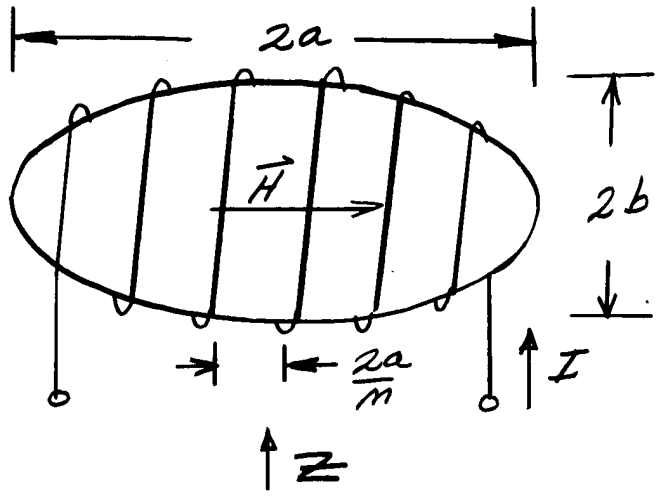

FIGURE D-1

when a current $$I = I_o \tag{D-1}$$

flows through the windings, a uniform magnetic field is established inside the core, directed along the axis, and having a magnitude

$$H_o = (1 - D)\frac{nI_o}{2a} \tag{D-2}$$

The total field consists of the linear superposition of the applied field and the demagnetization field.

$$\bar{H} = \bar{H}_o - D\bar{M} \tag{D-3}$$

The magnetization is defined as

$$\bar{M} = (\mu_{ir} - 1)\bar{H} \tag{D-4}$$

"D" is the demagnetization factor for the prolate spheroid[1]. Thus,

$$\vec{H} = (1 - D)\frac{nI_o}{2a} - D(\mu_{ir} - 1)H$$

or

$$H = \frac{(1 - D)\frac{nI_o}{2a}}{1 + D(\mu_{ir} - 1)} \qquad (D\text{-}5)$$

Then

$$\bar{B} = \mu_i \bar{H}$$

$$= \left[\mu_o \frac{\mu_{ir}}{1 + D(\mu_{ir} - 1)}\right](1 - D)\frac{nI_o}{2a}$$

$$= \mu_e (1 - D)\frac{nI_o}{2a} \qquad (D\text{-}6)$$

The induced voltage is[2]

$$e_i = -j\omega_o\left[\mu_e (1 - D)\frac{nI_o}{2a}\right]\left(\frac{n}{2a}\right) V \qquad (D\text{-}7)$$

The impedance is

$$Z = -\frac{e_i}{I_o}$$

$$= \left[j\omega_o \left(\frac{n}{2a}\right)^2 (1 - D)\, V\right]\mu_e$$

$$= \left[j\omega_o \left(\frac{n}{2a}\right)^2 V (1 - D)\right](\mu_e' - j\mu_e'')$$

$$= \left[\omega_o \left(\frac{n}{2a}\right)^2 V (1 - D)\right]\mu_e'' \qquad (D\text{-}8)$$

$$+ j\omega_o\left[\left(\frac{n}{2a}\right)^2 V (1 - D)\right]\mu_e'$$

$$= R + j\omega_o L$$

Therefore

$$R = \omega_o \left(\frac{n}{2a}\right)^2 V (1 - D)\mu_e'' \qquad (D\text{-}9)$$

$$L = \left(\frac{n}{2a}\right)^2 V (1 - D)\mu_e' \qquad (D\text{-}10)$$

APPENDIX E

THE EQUIVALENCE OF MAGNETIC AND ELECTRIC FIELD COUPLING BY LOOP ANTENNAS

Loop antennas are sometimes described as coupled to the magnetic field component in contrast to the electric field component[5]. Accordingly, the induced voltage is said to equal the time rate of change of magnetic flux linking the loop.

$$e_i = \frac{-d\phi}{dt} \qquad (E\text{-}1)$$

$$= \frac{-d}{dt} \int \bar{B} \cdot d\bar{A}$$

For the antenna shown in Figure E-1,

$$e_i = -j\,\omega\,\mu_o\,H_o\,A \qquad (E\text{-}2)$$

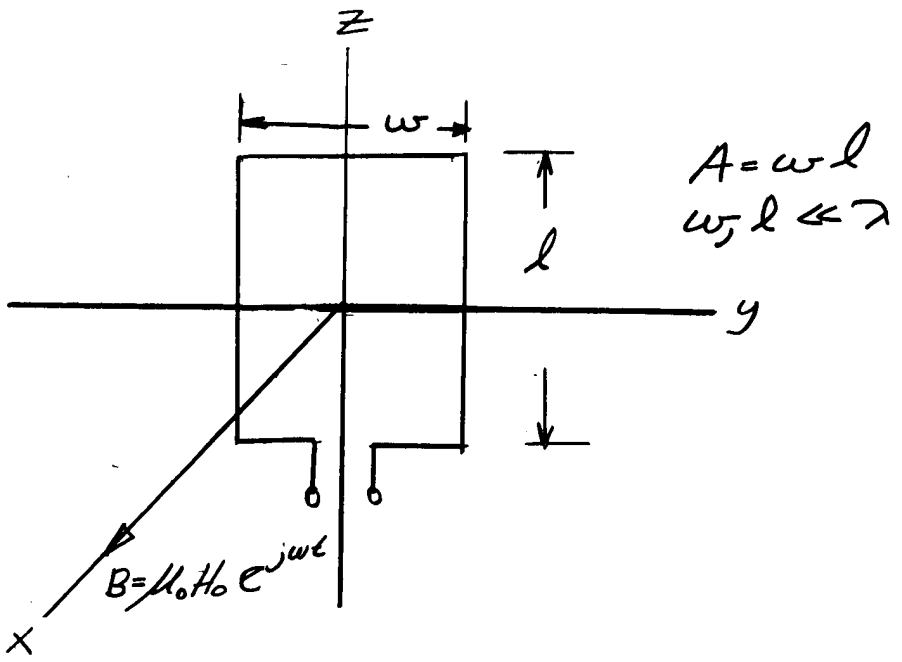

FIGURE E-1

However, the antenna can just as correctly be described as coupled to the electric field component. Then the induced voltage becomes

$$e_i = \oint \bar{E} \cdot d\bar{l} \qquad (E\text{-}3)$$

For the antenna shown in Figure E-2,

$$e_i = E_o \ell e^{-j\beta\frac{w}{2}} - E_o \ell e^{j\beta\frac{w}{2}}$$

$$= -2j E_o \ell \sin\frac{\beta w}{2} \qquad \text{(E-4)}$$

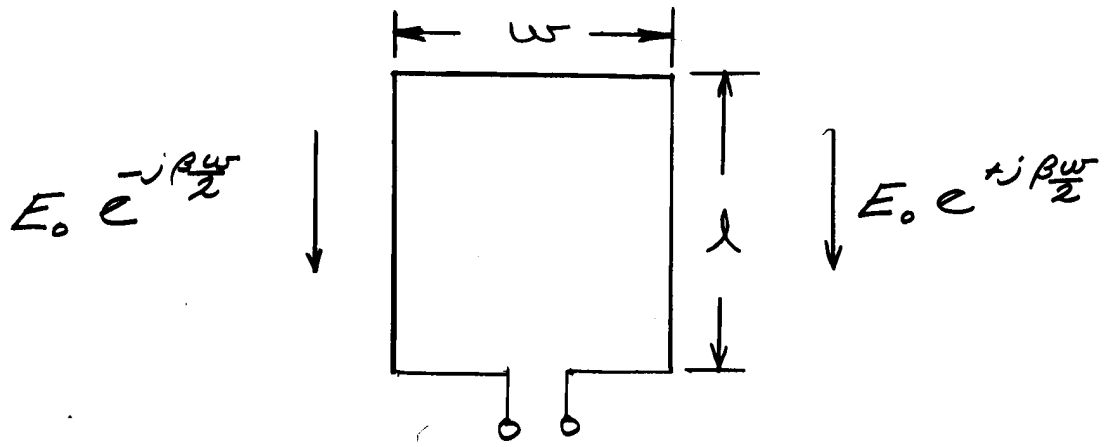

FIGURE E-2

The phase velocity is

$$\beta = \frac{2\pi}{\lambda}$$

For small antennas

$$\sin\frac{\beta w}{2} \approx \pi\frac{w}{\lambda} \qquad \text{(E-5)}$$

Then

$$e_i \quad \frac{-2\pi}{\lambda} j E_o A \qquad \text{(E-6)}$$

For a plane wave in free space

$$\lambda f = C$$

$$= \frac{1}{\sqrt{\varepsilon_o \mu_o}} \qquad \text{(E-7)}$$

and

$$E_o = \sqrt{\frac{\mu_o}{\varepsilon_o}} H_o \qquad \text{(E-8)}$$

The expression for the induced voltage becomes

$$e_i = -j \omega \mu_o H_o A \qquad \text{(E-9)}$$

Equations (E-2) and (E-9) are identical, illustrating that the loop antenna can be considered to couple either to the electric or to the magnetic field component with equal validity. The reader familiar with electromagnetic field theory will recognize the foregoing discussion as simple application of Maxwell's equation.

$$\vec{\nabla} \times \vec{E} = -\frac{\partial \vec{B}}{\partial t}$$

APPENDIX F

THE IMPEDANCE BANDWIDTH OF A PARALLEL RESONANT LRC CIRCUIT

A. CONSTANT INDUCTANCE

Consider the parallel resonant circuit in Figure F-1. The input impedance

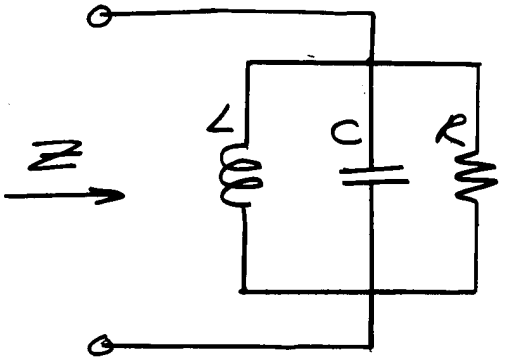

FIGURE F-1

is

$$Z = \frac{1}{1/R + j(\omega c - 1/\omega L)} \qquad (F-1)$$

Resonance occurs at

$$\omega_o C = 1/\omega_o L \qquad (F-2)$$

The impedance at resonance is

$$Z_o = R \qquad (F-3)$$

The impedance is 3 db down from its value at resonance for

$$(\omega_c C - 1/\omega_c L) = \pm 1/R \qquad (F-4)$$

The upper and lower 3 db cut-off frequencies are

$$\omega_{cu} = 1/2RC + \sqrt{(1/2RC)^2 + 1/LC} \qquad (F-5)$$

and

$$\omega_{cL} = -1/2RC + \sqrt{(1/2RC)^2 + 1/LC}$$

The 3 db bandwidth is

$$\triangle f = \frac{\omega_{cu} - \omega_{cL}}{2\pi}$$

$$= 1/2\pi RC \qquad \text{(F-6)}$$

B. $L = L_o/\omega$

The input impedance becomes

$$Z = \frac{1}{1/R + J(\omega_c + 1/L_o)} \qquad \text{F-7)}$$

The impedance still has its maximum value at resonance

$$Z_o = R$$

$$\omega_o C = 1/L_o \qquad \text{(F-8)}$$

The impedance is 3 db down from its maximum value at

$$(\omega_c C - 1/L_o) = \pm 1/R \qquad \text{(F-9)}$$

The upper and lower cuto-ff frequencies are

$$\omega_{cu} = 1/L_o C + 1/RC$$

$$\omega_{cL} = 1/L_o C - 1/RC \qquad \text{(F-10)}$$

The 3 db bandwidth is

$$\triangle f = 1/2\pi\ (\omega_{cu} - \omega_{cL})$$

$$= 1/\pi RC \qquad \text{(F-11)}$$